Postprint of: Bui V. G., Bui T. M. T., Tran V. N., Huang Z., Hoang A. T., Tarełko W., Bui V. H., Pham X. M., Nguyen P. Q. P., Flexible syngas-biogas-hydrogen fueling spark-ignition engine behaviors with optimized fuel compositions and control parameters, INTERNATIONAL JOURNAL OF HYDROGEN ENERGY, Vol. 48, iss. 18 (2023), pp. 6722-6737, DOI: 10.1016/j.ijhydene.2022.09.133

Flexible syngas-biogas-hydrogen fueling spark-ignition engine behaviors with optimized fuel compositions and control parameters

Van Ga Bui[1,*], Thi Minh Tu Bui[1], Van Nam Tran[1], Zuohua Huang[2], Anh Tuan Hoang[3,*], Wieslaw Tarelko[4], Van Hung Bui[5], Xuan Mai Pham[6], Phuoc Quy Phong Nguyen[7]

[1]*University of Science and Technology, The University of Danang, Vietnam*

[2]*State Key Laboratory of Multiphase Flow in Power Engineering, Xi'an Jiaotong University, Xi'an 710049, China*

[3]*Institute of Engineering, HUTECH University, Ho Chi Minh City, Viet Nam*

[4]*Faculty of Mechanical Engineering and Ship Technology, Gdańsk University of Technology, Poland*

[5]*University of Technology and Education, The University of Danang, Vietnam*

[6]*Mien Dong University of Technology, Vietnam*

[7]*PATET Research Group, Ho Chi Minh city University of Transport, Ho Chi Minh city, Vietnam*

** Corresponding authors:*

***Anh Tuan Hoang** (hatuan@hutech.edu.vn)*

***Van Ga Bui** (buivanga@ac.udn.vn)*

Graphic abstract

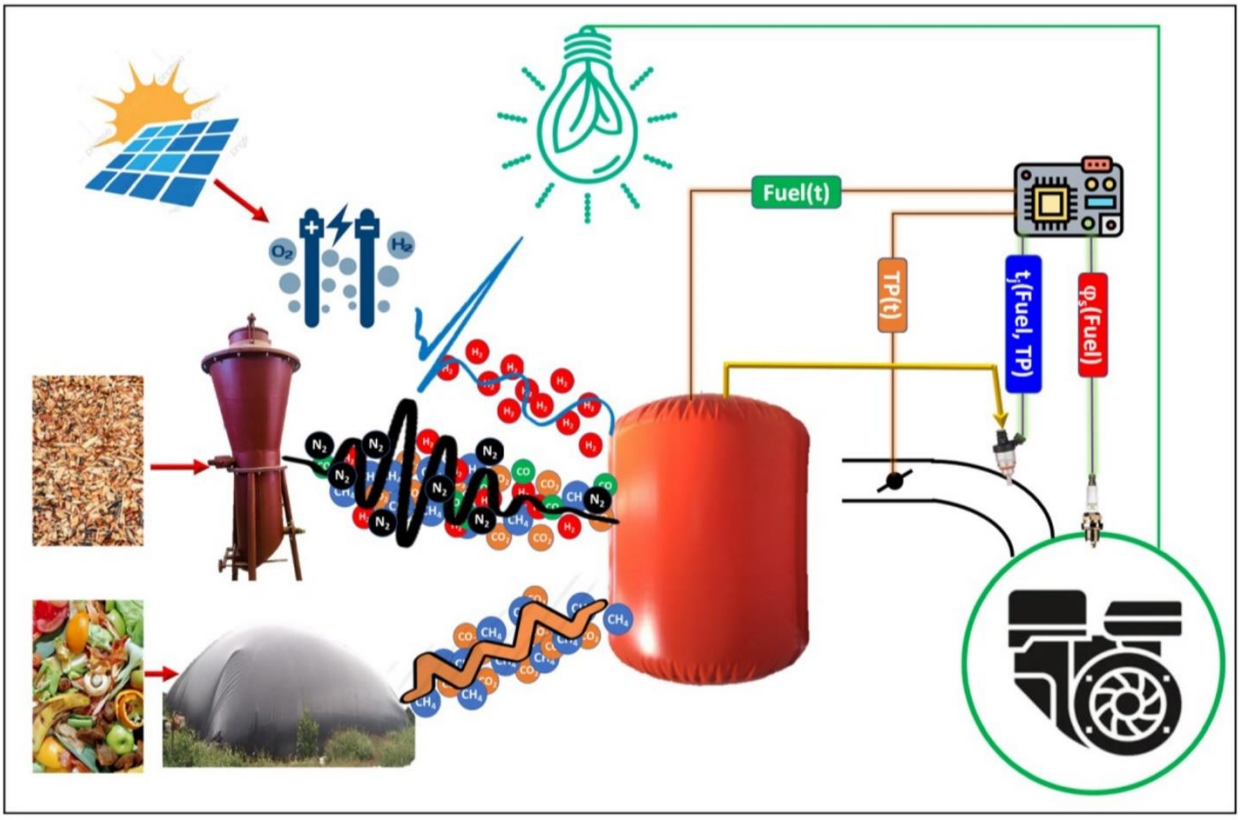

Abstract:

This paper presents the results research on the optimal fuel compositions and the control parameters of the spark ignition engine fueled with syngas-biogas-hydrogen for the purpose of setting up a flexible electronic control unit for the engine working in a solar-biomass hybrid renewable energy system. In syngas-biogas-hydrogen mixture, the optimal content of hydrogen and biogas is 20% and 30%, respectively. Exceeding these thresholds, the improvement of engine performance is moderate, but the pollution emission increases strongly. The optimal advanced ignition angle is 38°CA, 24°CA, and 18°CA for syngas, biogas, and hydrogen, respectively. With the same content of hydrogen or biogas in the mixture with syngas, the advanced ignition angle of the hydrogen-syngas blend is less than that of the syngas-biogas blend by about 4°CA at the engine speed of 3000 rpm. The derating power of the engine is 30% and 23% as switching from the hydrogen and biogas fueling mode to the syngas fueling mode, respectively. However, NO_x emission of the engine increase from 200 ppm (for syngas) to 2800 ppm (for biogas) and to over 6000 ppm (for hydrogen). The optimal advanced ignition angle, the optimal equivalence ratio of the syngas-biogas-hydrogen fuel mixture vary within the limits of the respective values for syngas and hydrogen. To improve the engine efficiency and reduce pollutant emissions, the loading control system of the engine should prioritize the adjustment of the fuel flow and then the adjustment of the air-fuel mixture flow.

Keywords: Hybrid renewable energy system; Biogas; Hydrogen; Combustion characteristics; Greenhouse gas emission; Flexible gaseous fuel spark-ignition engine

1. Introduction

In order to ensure that the increase in atmospheric temperature does not exceed 2°C compared to that of the pre-industry period by the end of this century, the emissions of greenhouse gases must be cut down right from now on [1][2]. To date, most countries around the world have committed to implementing the Paris Climate Agreement COP21 [3] in an effort to bring net emissions of greenhouse gases to zero by 2050 (Net-Zero) [4][5]. The transition from fossil energy to renewable energy is at the heart of the Net-Zero strategy [6][7], especially for the post-COVID19 pandemic [8][9]. Many countries have adopted policies that prioritize the development of clean energy; as a result, the share of renewable energy in power production worldwide has increased rapidly [10][11]. However, the use of a single source of renewable energy in general faces many technical challenges due to its low energy density, and random and discontinuous fluctuating power [12][13].

The hybrid renewable energy system (HRES), which combines the use of many different renewable energy sources, is an effective solution that helps to overcome these above inadequacies [14][15][16]. Compared with systems relying only on a single renewable energy source, HRES works stably with high reliability and reduces the need for energy storage [17][18]. The outstanding advantage of HRES is its low CO_2 emissions, which can be ignored compared to traditional fossil fuel power plants [19][20]. In addition, HRES can operate independently, so it can be easily applied in rural areas or remote areas without a national grid [21][22]. Countries in the tropical region, especially in South and Southeast Asia, abound in solar and biomass resources; therefore, solar-biomass HRES is rich in potential [23][24]. Combining the use of a randomly oscillating solar energy source with a controllable biomass energy source will ensure the continuous operation of the HRES system [25]. The average solar radiation in the region is at a high level, around 4-6 kWh/m^2/day [26]. On the other hand, this region is at the top of rice production in the world [27]; consequently, biomass from agricultural

waste accounts for a large proportion of renewable energy sources [28][29]. Wet biomass is suitable for biogas production through a biochemical process, while dry biomass is suitable for syngas production through thermochemical conversion [30][31]. Therefore, organic wastes can generally be separated into two streams: an easily biodegradable stream for biogas production and a hard biodegradable stream for syngas production [32][33]. In addition, in the solar-biomass HRES, when the capacity of the solar panels is higher than that of the load, the excess energy will be used to produce hydrogen through the water electrolysis process [34][35]. Syngas, biogas, and hydrogen are mixed together and fuel the engine that drives the generator. In the case of off-grid HRES, this engine-generator assembly is used as an energy storage system instead of batteries [36][37].

The composition of the HRES depends on the characteristics of the primary energy sources. These may include PV panels, wind turbines, hydro turbines, diesel generators, biogas generators, batteries, inverters, and a hydrogen storage system [38][39][40][41][42]. Today, most of these components can be easily found on the market, with the exception of syngas-biogas-hydrogen internal combustion engines. In fact, for a given fuel, all problems concerning the energy conversion efficiency such as advanced ignition angle, air/fuel ratio, and their relationships with the engine's performance and emissions need to be thoroughly examined before being applied in practice [43][44]. Although the internal combustion engine using fossil fuels has been applied for hundreds of years, research into this issue is still ongoing. The application of renewable fuels on engines requires thus more in-depth research, as they have only been put into use in recent years [45][46]. Therefore, internal combustion engines fueled with a syngas-biogas-hydrogen mixture, an important component of solar-biomass HRES, need to be thoroughly investigated.

In the literature, we can find separate studies on syngas engines [47][48]. Syngas can be used on dual-fuel engines or spark ignition engines [49]. The results of these studies showed

that when the engine is powered with syngas, the pollutant emissions are much lower than what is emitted when it is powered with traditional fuels [50]. CO and NO_x emissions in the case of syngas fueling mode are 30-96% and 54-84% lower, respectively than those in the case of the gasoline fueling mode [51]. However, due to the low calorific value of syngas, the engine power is significantly reduced [52]. In fact, when using syngas directly on natural gas engines, the engine power decreases from 20% to 30% [53][54]. A detailed evaluation of syngas engines is presented in the work of Fiore et al. [55]. To maintain engine power, one must enrich syngas with fuels of high calorific value such as natural gas, hydrogen, or fossil fuels [56]. In that case, syngas can be used as the main fuel or as an additive to other fuels [57].

Like syngas, biogas can be used as fuel for either dual fuel engines or spark ignition engines [58][59][60]. However, compared with syngas, biogas requires higher ignition energy and produces higher pollutant emissions [61]. Biogas contains the main components CH_4 and CO_2 with variable concentrations depending on input materials [62][63]. The increase in CH_4 concentration will improve the calorific value of biogas, resulting in an increase in combustion temperature and thermal efficiency [64]. However, under that condition, NO_x emissions also increase, so it is necessary to consider the relationship between energy efficiency and environmental pollution emissions upon the removal of CO_2 from biogas [65][66]. On the other hand, when the biogas engine operates with a poor mixture, the CO and NO_x emissions decrease and the thermal efficiency increases [67][68]. The optimal advanced ignition angle of stationary biogas engines increased as the CH_4 content in the fuel decreased. Yungjin et al. [69] studied the effect of CO_2 content in biogas on combustion characteristics and NO_x emissions of spark ignition engines and found that when the CO_2 concentration is increased, NO_x emissions decreased significantly under all operating conditions. CO_2 also improves the anti-knock properties of the fuel hence, biogas can be used in high compression ratio engines [62].

Unlike syngas and biogas, hydrogen has outstanding advantages such as high laminar flame speed, wide combustion limits, and low ignition energy, so the presence of hydrogen in the blends significantly improves the quality of combustion [70][71][72]. Due to the high combustion rate of hydrogen, the pressure curve peaks near the top dead center (TDC), increasing the maximum pressure compared to conventional fuels [73][74]. Even with a small amount of hydrogen, the fuel mixture can burn with a low equivalence ratio (ϕ), increasing the thermal efficiency of the engine [75][76]. When hydrogen is mixed into biogas, the engine can operate with a poor mixture [77][78]. This is because hydrogen can extend the flammability limits of the fuel blends [79]. Bui et al. [12][80] found that when the hydrogen content in biogas was increased, the advanced ignition angle (φ_s) decreased, and the indicative engine work cycle (Wi) increased slightly but NO_x emissions increased very significantly.

Even if the solar-biomass HRES does not produce hydrogen, the combined use of syngas and biogas from biomass is more efficient than the use of each component fuel in separation. In biogas, CH_4 has a high calorific value, and in syngas, hydrogen has a high burning rate. Therefore, with the employment of a mixture of syngas and biogas, the thermal efficiency of the engine can be maintained at the corresponding level of the component fuel, but NO_x emissions and detonation tendency decrease [64]. For both syngas and biogas, NO_x emissions are close to zero when poor mixtures are used [81]. Shivapuji et al. [72] analyzed the effect of hydrogen composition in biogas-hydrogen blends on the thermal efficiency of the engine. The authors found that the thermal efficiency of the engine increases from 18% to 24% when the hydrogen composition of the mixture increases from 7.1% to 9.5%. However, if the hydrogen composition in the blend is too high, the combustion process becomes unstable, and the maximum pressure increases too much causing detonation, so the thermal efficiency of the engine decreases [82]. The effect of hydrogen composition in the biogas-hydrogen blend on engine power was also examined by Park et al. with the variation of hydrogen content from 5

to 30% [83]. The authors found that when 5% of hydrogen is added to biogas, the engine efficiency increased by about 2%, but with the addition of 10% of hydrogen, the efficiency increased by about 0.8% compared to the value achieved with neat biogas fueling mode [83]. When hydrogen content increases, the combustion temperature increases, leading to an increase in heat loss for the coolant and NO_x emission [84][85]. Therefore, the hydrogen content is considered an important factor in adjusting the harmonization between performance and emissions of syngas-biogas-hydrogen fueling engines [45][64]. Besides the fuel compositions, φ_s also significantly affects the combustion quality. As for stationary biogas engines, the optimal φ_s depends on the fuel-air mixture composition. When the engine was powered by a fuel-air mixture with an equivalence ratio ϕ=0.8, the maximum thermal efficiency was achieved at the optimal φ_s of 30°CA and 35°CA respectively for methane and biogas [81]. For biogas containing 65% methane, the optimal φ_s is 30°CA and 45°CA, with ϕ of 1 and 0.7, respectively. For syngas, the optimal φ_s is in the range of 30°CA to 35°CA when ϕ=1 and increases to 40°CA when ϕ=0.8 [81]. With the same φ_s, the thermal efficiency of the syngas engine is higher, and the NO_x emissions are lower than the corresponding values of the biogas engine [64]. With regard to engines fueled with syngas, when hydrogen content increases, the thermal efficiency increases at a low advanced ignition angle but decreases at a large advanced ignition angle [77]. When the equivalence ratio is decreased, the NO_x concentration decreases but the thermal efficiency of the engine increases [44].

In brief, the impact of climate change and recent Europe's energy crisis shows the urgent need of changing from fossil energy to renewable energy for sustainable development [86][87]. Besides the perfection of solar plants [88][89], the energy conversion from biomass was improved by different technologies to be used efficiently in the solar-biomass HRES [90][91][92][93]. The large application of biomass offers interest not only in energy saving but also in reducing the investment cost of landfill gassing systems to control methane emission

[94][95][96]. As it has been mentioned above, the implementation of solar-biomass HRES needs the development of syngas-biogas-hydrogen engine. The literature research results showed the fundamental combustion characteristics of syngas, biogas and hydrogen-the basic fuel components powering the engine in the solar-biomass HRES. Syngas has a low calorific value which reduces engine power, but it produces very low pollutants [55][97]. Biogas has a higher calorific value than syngas but a low combustion rate and good resistance to detonation [98]. Hydrogen has a high combustion rate, and wide flammability limits, but it produces high NO_x concentration [99]. The reasonable selection of the fuel mixture compositions and the optimal organization of the combustion process are the main factors to ensure the highest efficiency and the lowest harmful emissions of the syngas-biogas-hydrogen fueling engine.

In the present-day market, it is difficult to find engines specifically designed to fuel syngas [100]. Engines fueled with syngas-biogas-hydrogen mixtures suitable for solar-biomass HRES are still harder to find, even research related to this engine is still very rare in the literature. Published works related to this field have only mentioned the performance and emissions of engines using separately syngas, biogas, or biogas, syngas enriched with methane, and hydrogen. This paper focuses on studying the combustion characteristics of the syngas-biogas-hydrogen blends with flexible compositions, suitable for engines working in solar-biomass HRES. This helps to fill the gap in the literature concerning flexible gas-fueled engines. The main purposes of the work are to identify the optimal fuel mixture compositions and the optimal operating parameters of the syngas-biogas-hydrogen fueling engine. These are the new points of the present work. The results will orient the engine control system in such a way as to improve efficiency and reduce the pollutant emissions of the engine. The development of control technology based on the research is beneficial not only to the new engine production but also to the conversion of traditional engines into syngas-biogas-hydrogen flexible fuel

engines. The availability of these engines contributes to the large application of solar-biomass HRES.

2. Material and method

2.1. Engine and fuels

The study was performed on a syngas-biogas-hydrogen stationary engine converted from the Honda GX200 spark-ignition engine. The engine has a cylinder diameter of 68mm, a piston stroke of 45mm, and a compression ratio of 8.5. It is a carburetor fueling, magneto ignition traditional engine. It generates a maximum power of 4.8 kW at 3600 rpm in gasoline fueling mode.

Table 1. Properties of fuels

Fuel	Compositions (mol/mol)					M (g/mol)	m_{air}/m_{fuel} (g/g)	V_{air}/V_{fuel} (l/l)
	CH_4	H_2	CO	CO_2	N_2			
Biogas	0.7	0	0	0.3	0	24.40	7.98	6.71
Syngas	0.05	0.18	0.20	0.12	0.45	24.64	1.64	1.39
Hydrogen	0	1	0	0	0	2	34.78	2.4
Low calorific value (MJ/Nm^3)	33,906	10,246	12,035	-	-			

Table 2. Blend compositions

Blend	Volumetric composition (%)		
	Syngas	Biogas	Hydrogen
Blend1	60	20	20
Blend2	40	40	20
Blend3	20	60	20
Blend9	50	0	50
Blend11	80	20	0
Blend12	70	30	0
Blend13	60	40	0
Blend14	50	50	0

The main properties of the fuels were presented in **Table 1**. Biogas-syngas-hydrogen blends with different compositions used in the study were introduced in **Table 2**. With the given gas composition in the fuel, the mass molar, gravimetric m_{air}/m_{fuel}, and volumetric V_{air}/V_{fuel} can

be calculated. Besides, the heat value of the fuel can be determined through the heat value of its components.

2.2. Method

The study was performed by means of numerical simulation with the help of CFD software ANSYS Fluent 2021R1. The Honda GX200 engine was converted into the syngas-biogas-hydrogen engine with a retrofitted intake manifold. The calculation space was designed by SolidWork software. The meshing of the cylinder, combustion chamber, and intake manifold was generated automatically with different element geometry and dimension. Dynamic meshing was applied for the cylinder space due to the variation of the piston position. The grid independency was analyzed to identify the optimal number of cells used in the simulation. The details of the model setup were presented in our previous work [80].

In this work, the Re-Normalized Group RNG k-ε model was used to describe the turbulence phenomena. The combustion of the syngas-biogas-hydrogen mixture with air was calculated through the Partially Premixed Combustion model. In this model, the front of the flame is determined by the mean value of the reaction progress variable c. In the combustion products c=1 and the fresh mixture c=0. The combustion products were calculated via the mean value and the variance of mixture fraction f [80]. The extended Zeldovitch mechanism was applied to simulate the NO_x formation [70]. CO emission was determined through the thermodynamic equilibrium of combustion products.

The input parameters for boundary conditions include the temperature of the fuel, the temperature of the air, the gauge pressure of fuel injection, gauge pressure of intake air. The mixture fraction f=0 at the entrance of the intake manifold and f=1 at the entrance of the fuel injector. The reaction progress variable c=0 for fresh gas and mixture and c=1 for combustion products. The resolution of the governing equations was described in [80][101].

3. Results and discussion

3.1. Effects of fuel composition and equivalence ratio

Fig. 1a compares the variation of the heat release rate (HRR) according to the crankshaft angle (CA) when the engine was fueled with a stoichiometric mixture of biogas, syngas, and Blend12, operating at speed of 3000 rpm. Because syngas is very poor with a low combustion rate, the maximum HRR of syngas is only 65% compared to that of biogas. The peak of biogas' HRR curve is 10°CA earlier than that of syngas. The maximum in-cylinder pressure (P_{max}) in the syngas fueling case is only 23 bar, compared to 35 bar in the biogas fueling case. The capacity of the syngas engine is thus lower than that of the biogas engine as mentioned by Pradhan et al. [52]. When 30% of biogas is added to syngas (Blend12), the maximum HRR of the blend is nearly 90% of that of biogas, i.e., it increases by 25% compared to that of syngas. Consequently, the maximum pressure and the maximum temperature (T_{max}) in the case of Blend12 fueling mode is 5 bar and 150K higher than the corresponding value of syngas fueling mode (**Fig. 1b**) and (**Fig. 1c**).

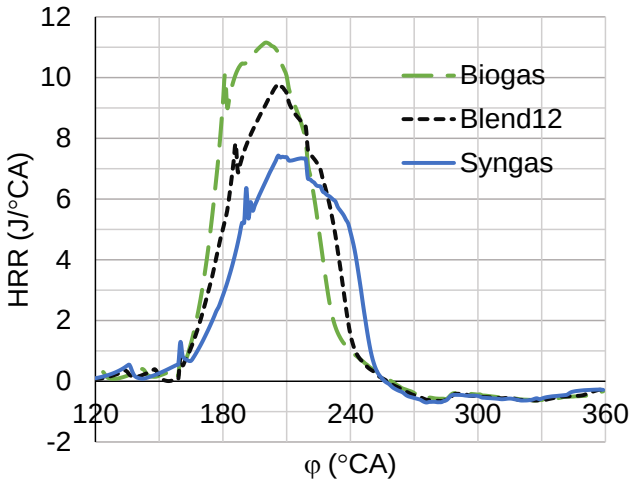

(a)

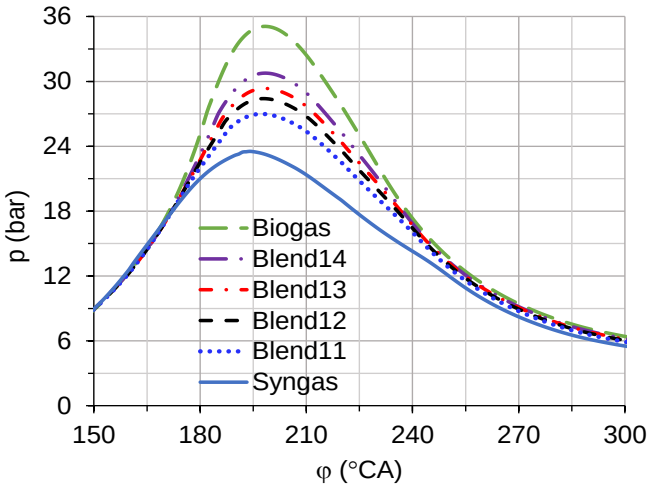

(b)

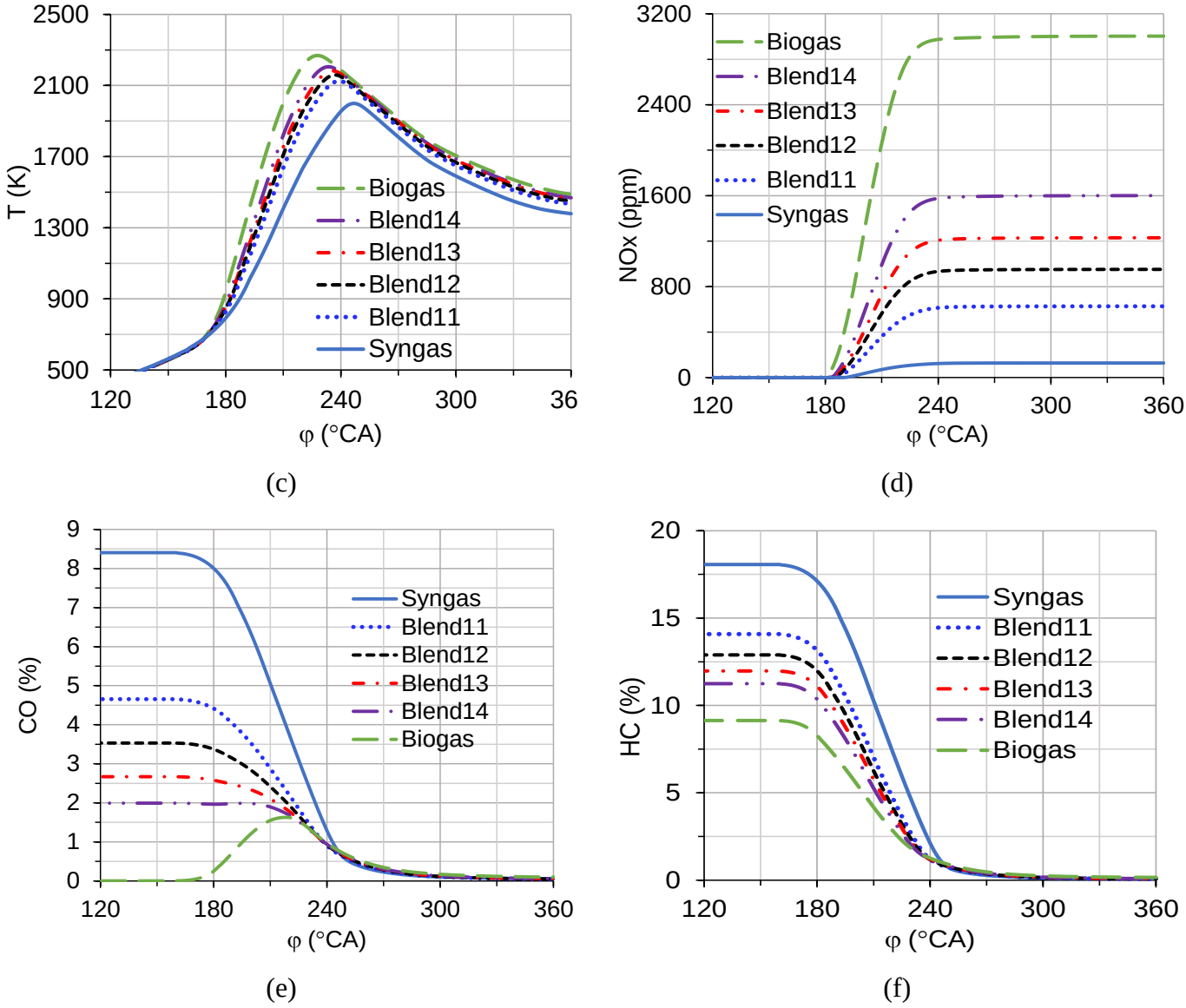

Fig. 1. Comparison of variations of combustion characteristic parameters with crankshaft angle when the engine was fueled with syngas, biogas, and blends (n=3000 rpm, ϕ=1, φ_s=20°CA); (a) HRR, (b) Pressure, (c) Exhaust gas temperature, (d) NO_x emission, (e) CO emission, (f) HC emission

The maximum combustion temperature of the syngas fueling case is about 300K lower than that of the biogas fueling case. This is due to the low calorific value of the syngas. However, the low-combustion temperature of syngas results in an extremely low level of NO_x emission compared to biogas. This result confirms the observation of Sharma et al. [50]. **Fig. 1d** showed that NO_x concentration in the case of the biogas fueling mode was nearly 20 times higher than that of the syngas fueling mode. Because syngas contains CO, the initial CO

concentration in the fresh mixture is much higher than that of biogas (Figure 1e). During combustion, CO concentration results from the thermodynamic equilibrium of combustion products. Due to the V_{air}/V_{fuel} ratio of CO and H_2 being both smaller than that of CH_4, the total HC concentration in the fresh mixture for syngas is nearly twice as high as in the case of biogas (**Fig. 1f**). There is practically no significant effect of fuel compositions on the CO and HC emissions in stoichiometric combustion.

A general comparison of combustion characteristics of syngas, biogas, and syngas-biogas blends is presented in **Fig. 2a**. As it has been mentioned above, when ϕ=1, the concentrations of CO and HC were very low. They tend to decrease slightly with the increase in biogas content in the mixture with syngas. CO concentration varies in the range of 0.047%-0.059% and HC varies in the range of 0.096 - 0.127%. Two important characteristics in the comparison are W_i and NO_x emission. The results show that W_i reaches 186 J/cyc for biogas and 149 J/cyc for syngas, thus, W_i decreased by nearly 20% when switching from the biogas fueling mode to the syngas fueling mode. This power derating is lower than that compared to the natural gas fueling mode according to the report of Sridhar et al. [53]. However, NO_x emission in the case of the syngas fueling mode is only about 180 ppm, neglected before 3820 ppm in the case of biogas. As compared to the gasoline engine, NO_x emission of the syngas engine can be reduced by more than 84% [51]. **Fig. 2b** shows the $W_i(NO_x)$ relationship among different biogas contents in the mixture with syngas. When the biogas composition is less than 30%, W_i increases faster than NO_x, but when biogas content exceeds this threshold, W_i increases insignificantly while NO_x increases strongly. The addition of biogas into syngas improves thus, indicative engine work cycle, but leads to a strong rise in NO_x concentration in the exhaust gas. The harmonizing ratio W_i/NO_x can be obtained with 30% biogas in the mixture with syngas.

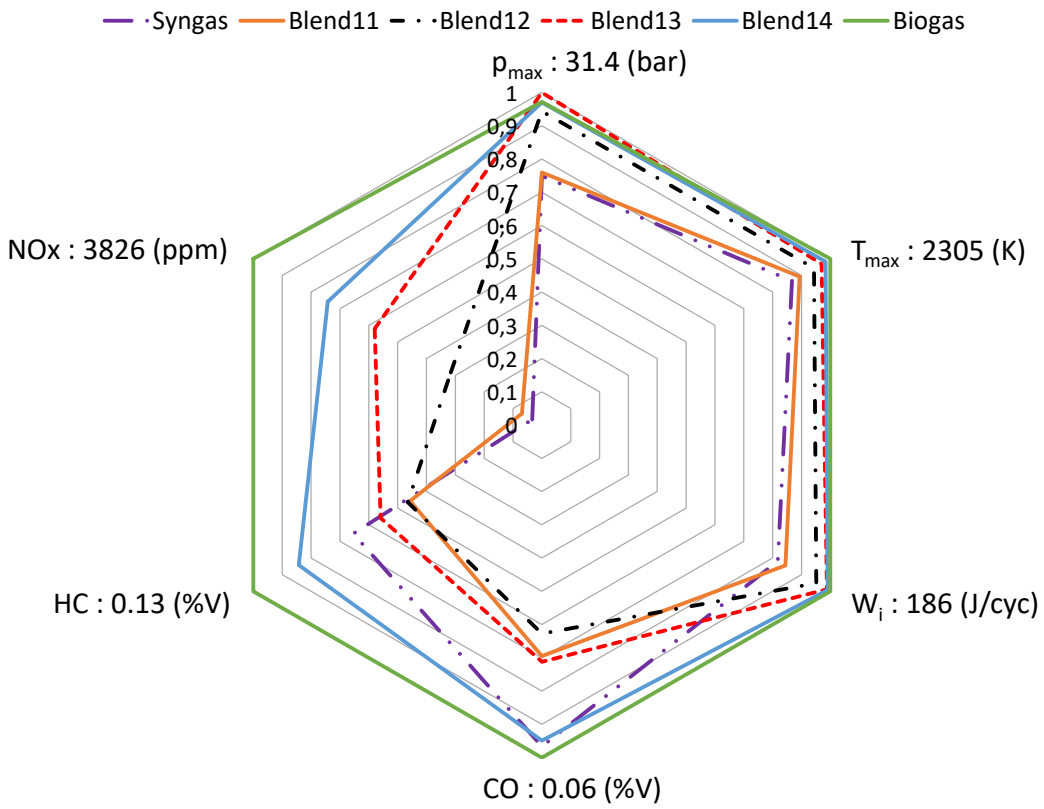

(a)

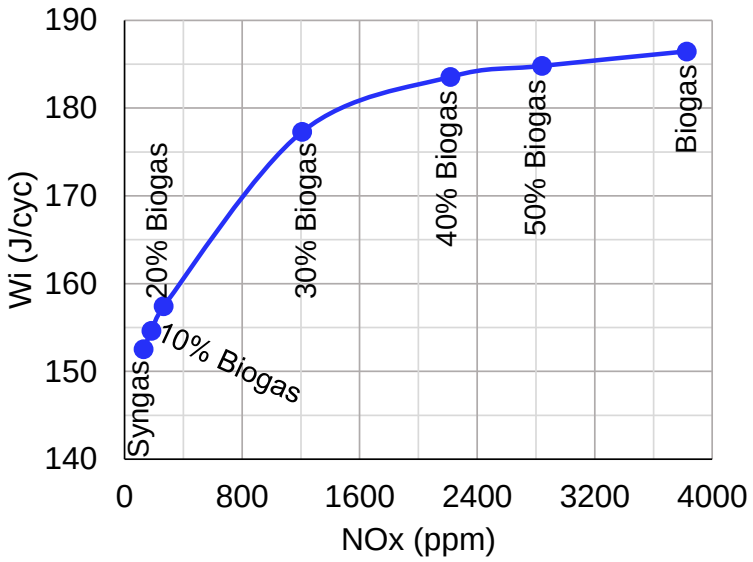

(b)

Fig. 2. Comparison of performance and emission of the engine fueled with syngas-biogas blends and with fuel component, operating at speed of 3000 rpm, ϕ=1, φ_s=20°CA; (a) Effects of fuel compositions on P_{max}, T_{max}, W_i, concentrations of CO, HC, NO_x; (b) Relationship W_i-NO_x)

Similar simulation calculations were performed for the syngas-hydrogen mixture. As mentioned in the introduction, hydrogen has a much higher combustion rate than that of biogas or syngas [70][71][72]; therefore, when it is blended with these fuels, the combustion process is improved. **Fig. 3** presents the summary variations of W_i, T, CO, HC, and NO_x with hydrogen composition in the syngas-hydrogen blend, at engine speed n=3000 rpm, ϕ=1, and φ_s=23°CA. The results showed that as the hydrogen concentration is lower than 10%, the combustion characteristic parameters have not changed much compared to syngas. W_i increases sharply as the hydrogen concentration varies from 10% to 20%. When the hydrogen concentration exceeds the 20% threshold, W_i increases slowly because the effect of hydrogen on the combustion improvement is not considerable. In the case of the biogas engine, the enrichment of 10% hydrogen is reasonable [72][83]. This threshold is lower than that in the case of syngas enriched by hydrogen because syngas is much poorer than biogas.

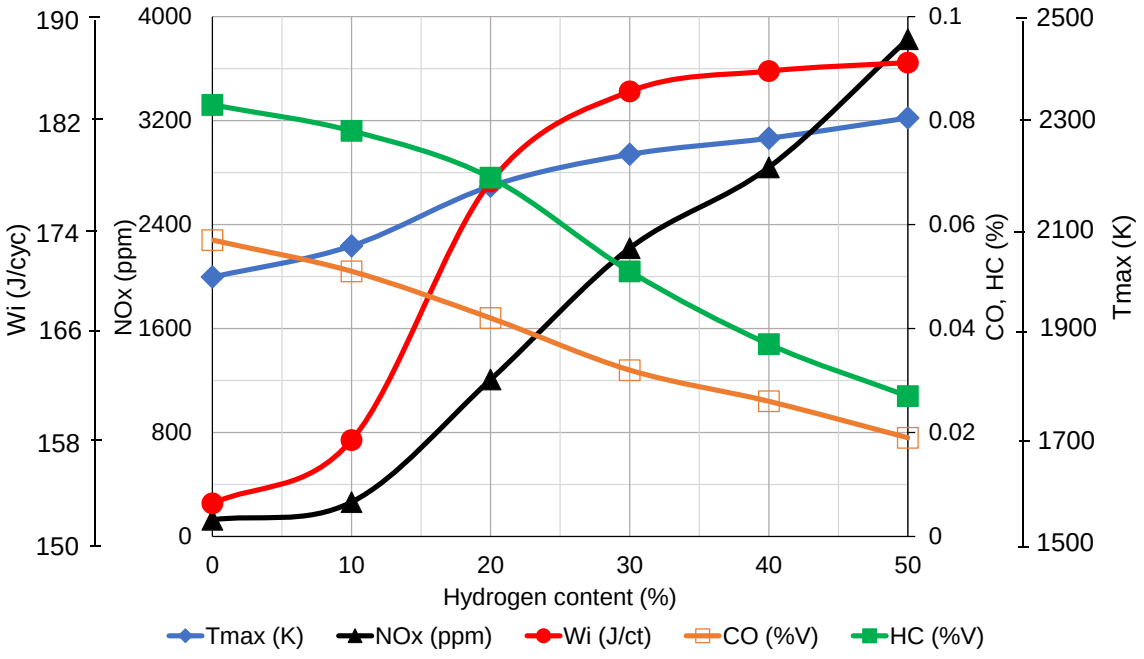

Fig. 3. Variations of W_i, T_{max}, and pollutants concentrations with hydrogen content in the syngas-hydrogen blend (n=3000 rpm, ϕ=1, φ_s=20°CA)

It can be seen in **Fig. 3** that NO_x emissions increased almost linearly with the hydrogen content in the mixture with syngas due to the increase in combustion temperature. When 50% hydrogen is mixed into syngas, W_i increases by 22%, but the concentration of NO_x in the exhaust gas increases up to 20 times compared respectively to those of the neat syngas fueling mode. Meanwhile, if 20% of hydrogen is mixed into the syngas, W_i would increase by 17%, and the NO_x concentration would only increase 7 times compared respectively to those of the neat syngas fueling mode. The concentrations of CO and HC tend to decrease with the increase in hydrogen content in the syngas due to the fact that combustion takes place more completely. Hence, to harmonize the performance and emissions of the engine, the addition of 20% hydrogen in the mixture with syngas is optimal.

Fig. 4a introduces pressure curves of Blend1, Blend2, and Blend3 containing syngas, biogas, and hydrogen. In these blends, the hydrogen component is fixed at an optimal value of 20%, and the biogas component increases from 20% to 40%. It can be seen that when the biogas composition increases from 20% to 40%, P_{max} increases from 27 bar to 32 bar. Meanwhile, if the biogas composition increases from 40% to 60%, P_{max} increases only from 32 bar to 33 bar. The results showed that the effects of biogas on the combustion of the blend are more significant when the biogas content is low. When biogas dominates the fuel blends, the CO_2 impurities in the mixture account for an almost stable proportion. Therefore, the change in the biogas composition did not significantly change the ratio of HC over the total impurities CO_2 and N_2. **Fig. 4b** shows that the peak of heat release rate increases proportionally with the maximum pressure P_{max}. When the engine is fueled with syngas, the heat release rate is low, and the peak of the HRR curve shifts towards the expansion stroke, reducing P_{max} and W_i (**Fig. 4b**).

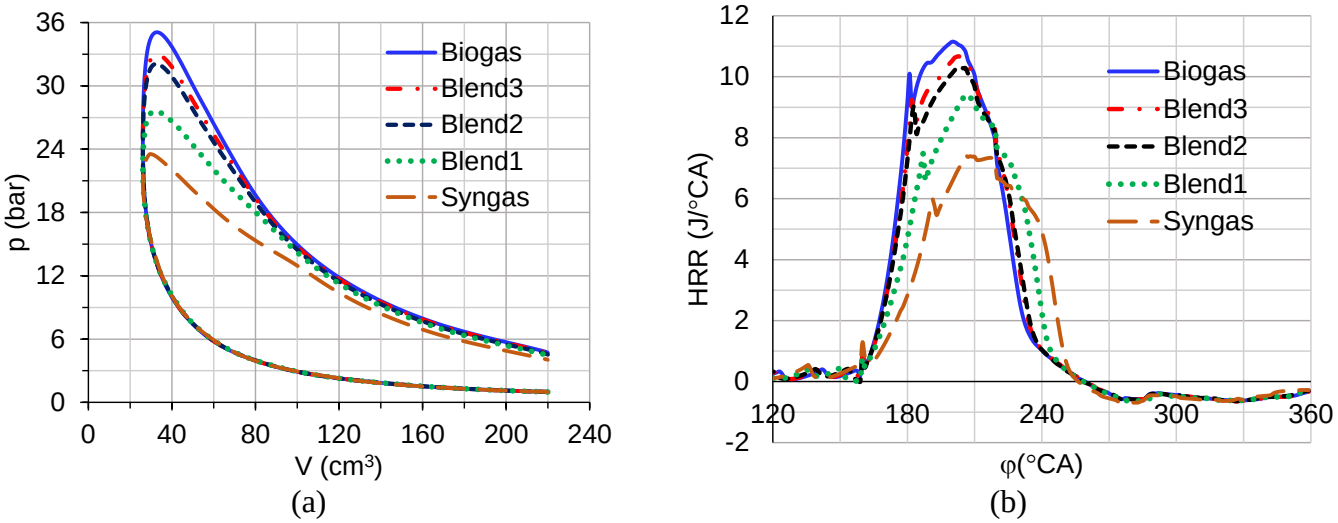

Fig. 4. Variations of pressure and HRR according to crankshaft angle under effects of fuel compositions (n=3000 rpm, ϕ=1, φ_s=20°CA; (a) Variation of pressure; (b) Variation of HRR)

Fig. 5 compares the combustion characteristics of the syngas-biogas-hydrogen fueling engine under the effects of fuel compositions. The characteristic parameters of combustion were highest for biogas and lowest for syngas. The results show that Blend2 gives W_i approximately Blend3, but concentrations of pollutants are lower than those of Blend3. When a switch is made from Blend1 to Blend2, the NO_x concentration increases from 1300ppm to 1600ppm, i.e., increasing 300ppm. However, when a switch is made from Blend2 to Blend3, the NO_x concentration increases by 1200ppm. When 20% of hydrogen and 20% of biogas is added to the mixture with syngas, W_i increases by 18%, and NO_x increases by 40% compared to the neat syngas fueling mode. When 40% of biogas and 20% of hydrogen is added into syngas, W_i increases by 20%, and NO_x increases by 50%. Thus, with a given hydrogen content in the mixture, W_i and NO_x concentration increase along with an increase in biogas concentration in the fuel blends.

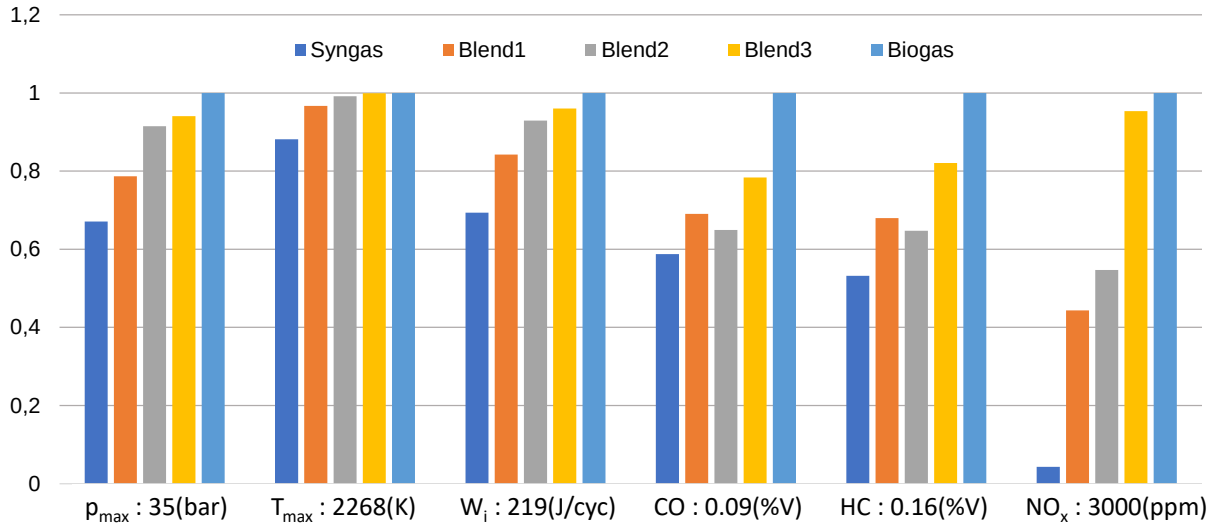

Fig. 5. Effects of fuel compositions on P_{max}, T_{max}, W_i and pollutants emissions of the engine fueled with syngas, biogas, and syngas-biogas-hydrogen blends (n=3000 rpm, ϕ=1, φ_s=20°CA)

Fuel-air mixtures can burn when the equivalence ratio is within the flammability limits, i.e., between the minimum and the maximum equivalence ratios. With regard to CH_4, the flammability is in the range of 0.8-1.6. Meanwhile, regarding H_2, the corresponding flammability is in the range of 0.3-2.3. **Fig. 6a** and **Fig. 6b** present the effects of ϕ on the variations of p and T with crankshaft angle. The engine was fueled with Bend2, operating at speed of 3000 rpm. It can be seen that P_{max} and T_{max} were achieved with an equivalence ratio slightly larger than the stoichiometric value. **Fig. 6c** shows that when ϕ<1, the CO emissions are almost zero, but it increases strongly ϕ when ϕ>1. **Fig. 6d** presents the effect of ϕ on the NO_x variation with the crankshaft angle. It can be seen that NO_x emission depends on combustion temperature, thus the largest NO_x concentration is found around the stoichiometric value of ϕ. NO_x concentration is very low with a poor mixture due to low combustion temperature.

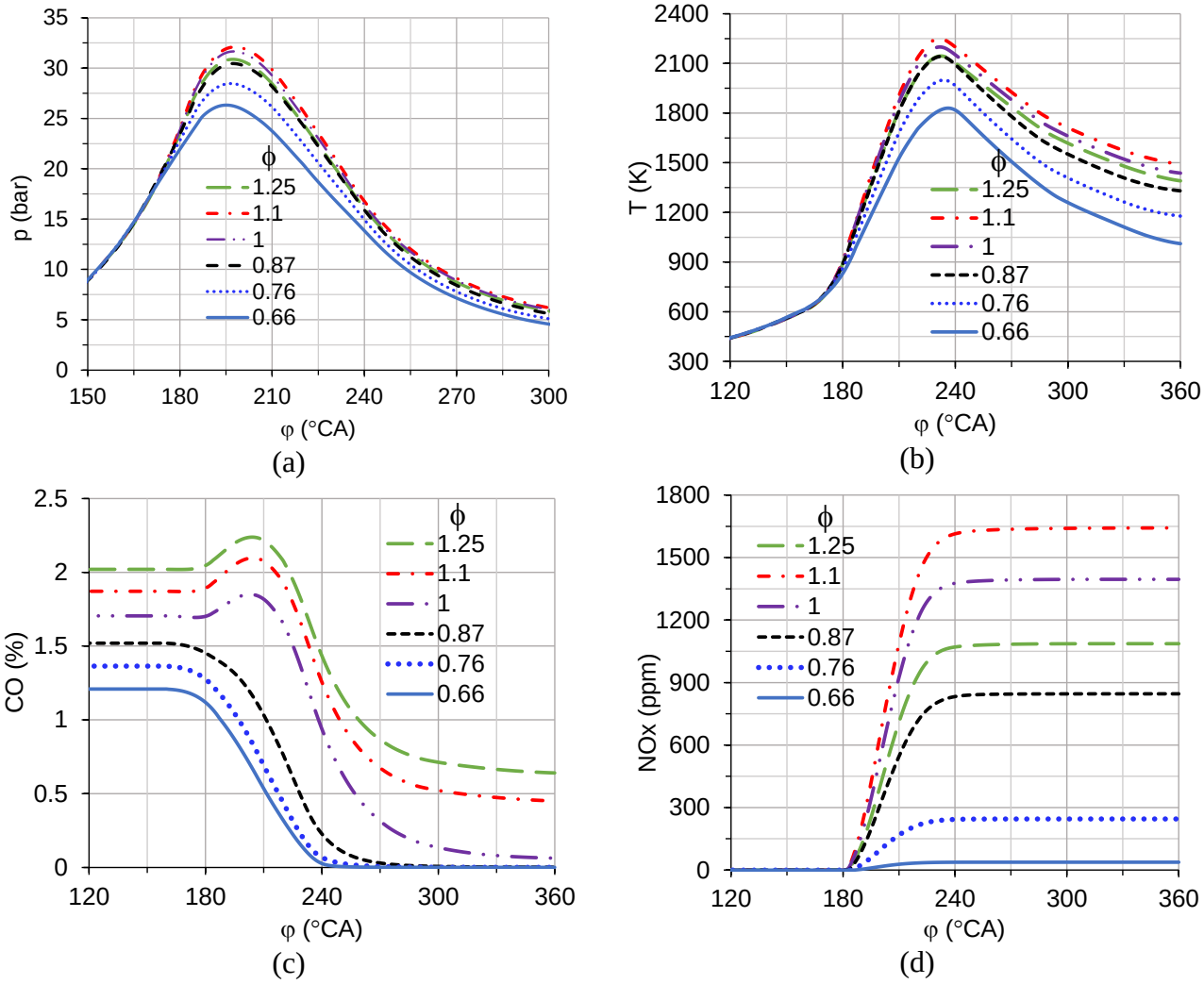

Fig. 6. Effect of ϕ on variations with crankshaft angle (Blend2, n=3000rpm and φ_s=20°CA); (a) pressure, (b) temperature, (c) CO concentration, (d) NO_x concentration

Fig. 7 shows that the $W_i(\phi)$ curve has a peak value corresponding to the optimal equivalence ratio ($\phi_{optimal}$). At $\phi_{optimal}$, the pressure, as well as the combustion temperature, reached the maximum values. **Fig. 8** shows that when the content of hydrogen or biogas in the mixture with syngas increases, $\phi_{optimal}$ tends to get closer to the stoichiometric value. With the same content of hydrogen or biogas in the mixture with syngas, $\phi_{optimal}$ of the syngas-biogas mixture is higher than that of the syngas-hydrogen mixture. Thus, the addition of hydrogen into

syngas is more beneficial for CO and HC reductions because these pollutants depend strongly on the equivalence ratio.

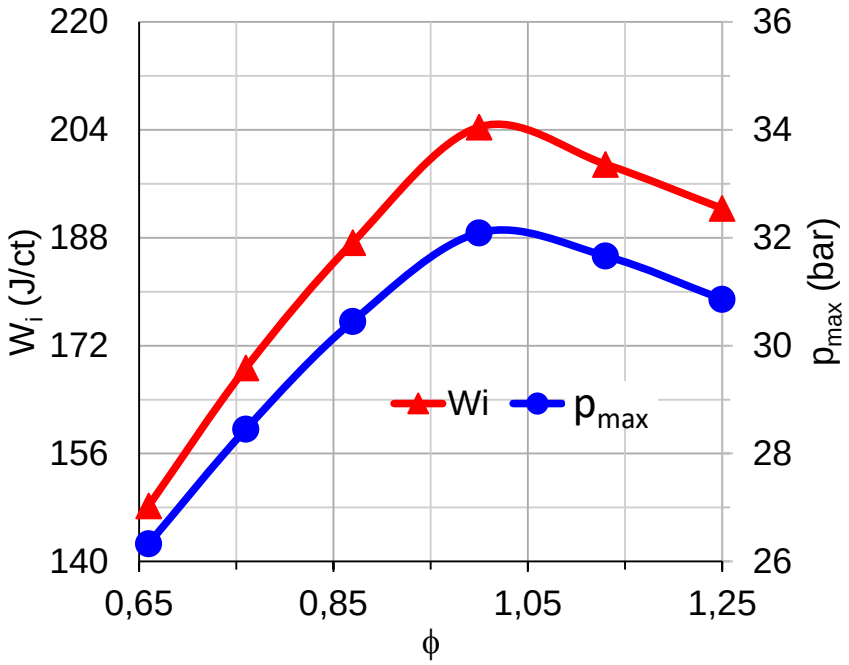

Fig. 7. Variations of Wi and P_{max} with ϕ (Blend2, n=3000rpm and φ_s=20°CA)

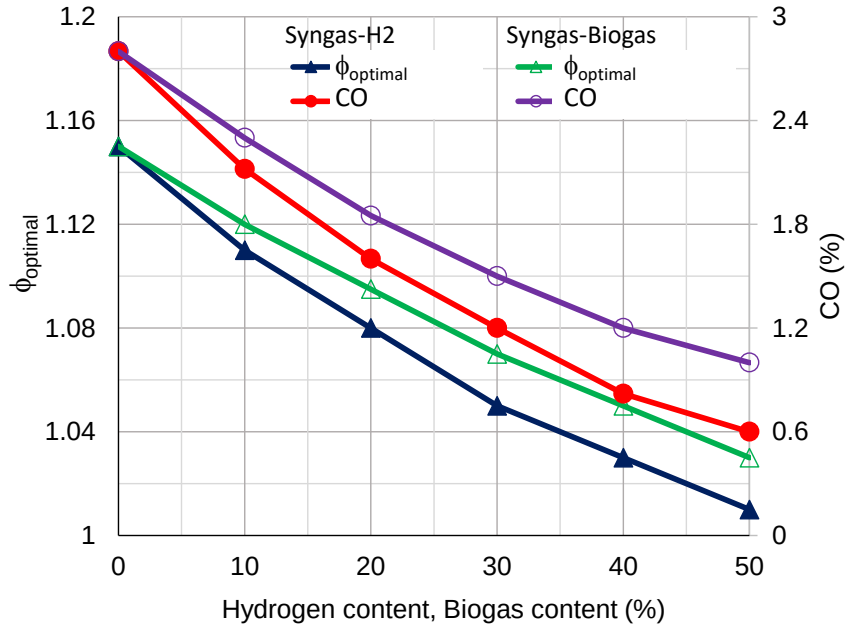

Fig. 8. Variation of $\phi_{optimal}$ and CO concentration according to hydrogen, and biogas contents in the mixture with syngas (n=3000rpm and φ_s=20°CA)

The above results showed that the richer the mixture is, the more disadvantageous the control of pollution is. The advantage of the combined use of different fuels is that the combustion process can be achieved with a mixture as poor as possible. Due to wide combustion limits, hydrogen can improve the combustion of low equivalence ratio mixture. This property enables the control of the loading regime of the engine by adjusting the equivalence ratio instead of adjusting the mixture flow.

Fig. 9 shows that to obtain an indicative engine work cycle around 165 J/cyc, for Blend1 and Blend2, we can adjust either the equivalence ratio or the mixture flow rate. When ϕ decreases to 0.78 for Blend1 or 0.8 for Blend2, the emissions of CO and HC are practically null, and the emission of NO_x is lower than 250 ppm. While the loading regime (corresponding to fuel-air mixture flow rate) decreases to 78% for Blend1 or 76% for Blend2, the CO emission is in the range of 0.36%-0.54%, the emission of HC is in the range 0.7 - 1% and the emission of NO_x is in the range 1100 ppm-1200 ppm. To obtain the same W_i under partial load and $\phi_{optimal}$, when the engine is fueled with Blend12 and Blend14, CO and HC emissions are significantly higher, approximately doubling the corresponding values of Blend1 and Blend2 while NO_x emission is in the same range. Thus, to obtain the same engine power, the syngas-hydrogen fuel mixture is more beneficial than the syngas-biogas mixture with regard to pollutant emissions.

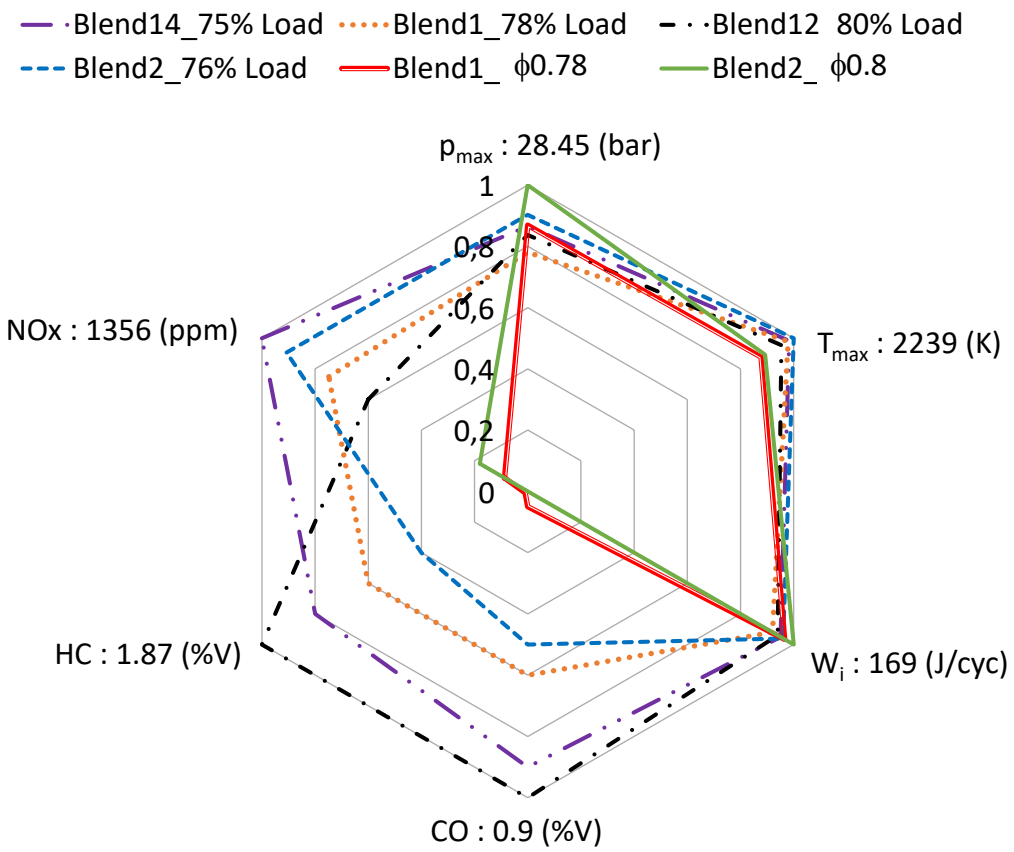

Fig. 9. Effect of loading regime and equivalence ratio on combustion characteristics of the engine fueled with variable compositions of syngas-biogas-hydrogen blends (n=3000 rpm, φ_s=20°CA)

In order to improve the efficiency of the combustion and reduce pollutant emissions, the loading of the engine fueled with syngas-biogas-hydrogen blends should be controlled by both mixture quality (via the equivalence ratio) and mixture quantity (via the air-fuel mixture flow rate). The control system should first and foremost prioritize the adjustment of the fuel flow and then the adjustment of the air-fuel mixture flow rate. This concept is a target of the special electronic control unit for syngas-biogas-hydrogen engines.

3.2. Effects of the advanced ignition angle

Fig. 10a presents the effects of advanced ignition angle φ_s on the variation of in-cylinder pressure, temperature and heat release rate of engines fueled with a stoichiometric mixture of

Blend2. When φ_s increases, the HRR curve increases earlier, P_{max} position approaches the TDC. This results in an increase in maximum pressure as well as the maximum combustion temperature. The result shows that when φ_s increases from 20°CA to 32°CA, P_{max} increases from 32 bar to 37 bar. When P_{max} appears earlier, the energy loss for the compression increases, thus W_i does not vary proportionally to P_{max}. In the case of φ_s=20°CA, the combustion temperature in the combustion stage is higher, but the product temperature during the expansion process is lower than the corresponding temperature of the case φ_s=32°CA. The rise in combustion temperature is accompanied by an increase in the existing time of combustion products in a high-temperature medium when increasing the advanced ignition angle, resulting in an increase in NO_x emission [102]. Concretely, NO_x concentration increases from 2100 ppm to 2800 ppm when φ_s increases from 20°CA to 32°CA (**Fig. 10b**).

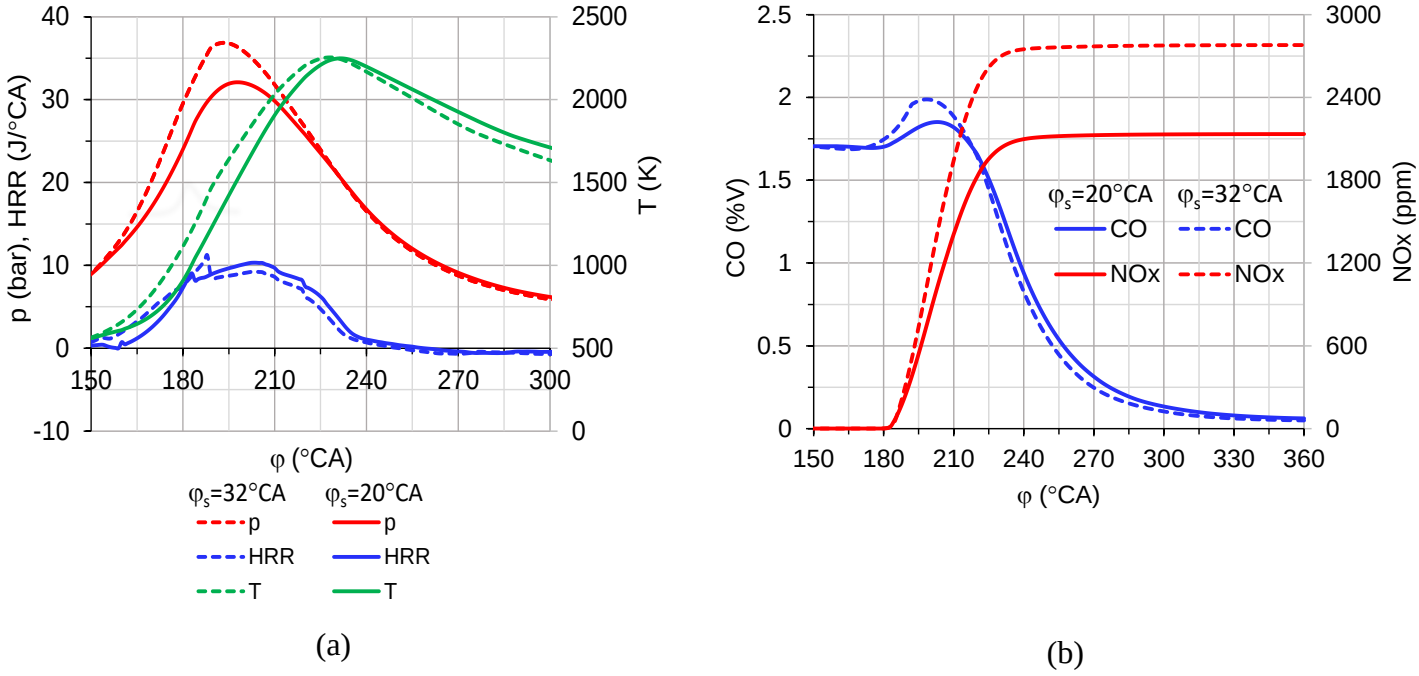

(a) (b)

Fig. 10. Variations of p, T, HRR, and pollutant emissions according to crankshaft angle under effects of advanced ignition angle: (a) Variation of pressure, temperature, and HRR; (b) Variation of CO and NO_x concentrations (Blend2, ϕ=1, n=3000 rpm)

Fig. 11a and **Fig. 11b** show the effects of biogas and hydrogen contents in the blend with syngas on the variation of W_i according to φ_s. With a given hydrogen or biogas content, the curve of indicative engine cycle work has a maximum value corresponding to the optimal advanced ignition angle (φ_{sop}). W_i increases, but the optimal φ_s tends to decrease with the increase in biogas or hydrogen content in the blend with syngas. This is due to the fact that when syngas is substituted with hydrogen or biogas, the fuel energy introduced into the cylinder as well as the combustion rate increases, which improves the engine performance and reduces the combustion time [103]. When φ_s is increased, the peak of the HRR curve tends to move to the TDC, resulting in an increase in the maximum temperature. Furthermore, the existing time of combustion of products in a high-temperature medium is extended with an increase in φ_s. The concentration of NO_x in the combustion mixture thus increases significantly with the increase in hydrogen or biogas content as shown in **Fig. 11c** and **Fig. 11d**.

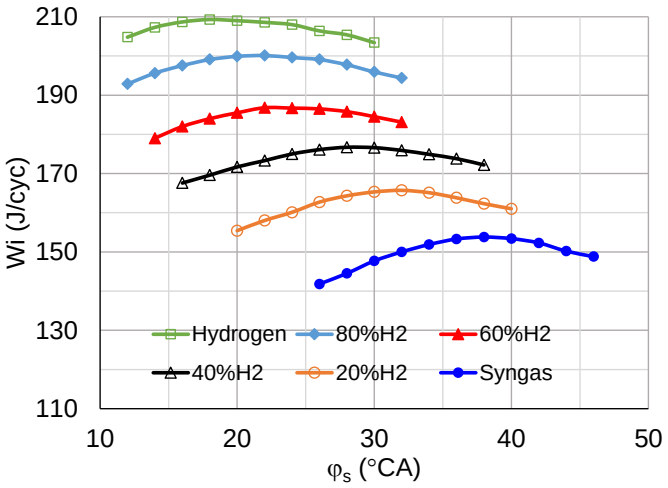

(a)

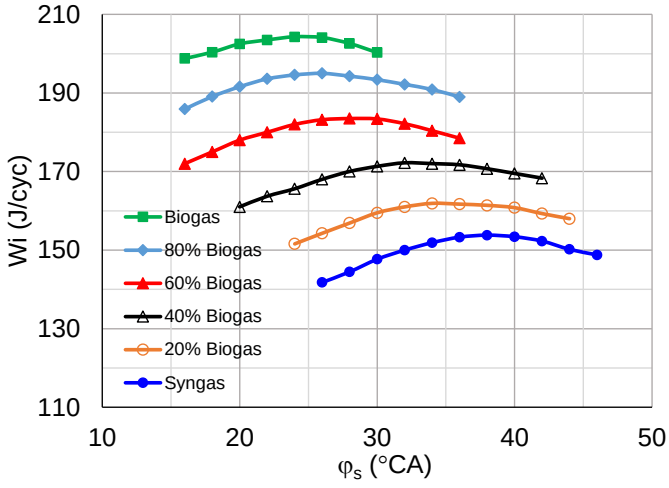

(b)

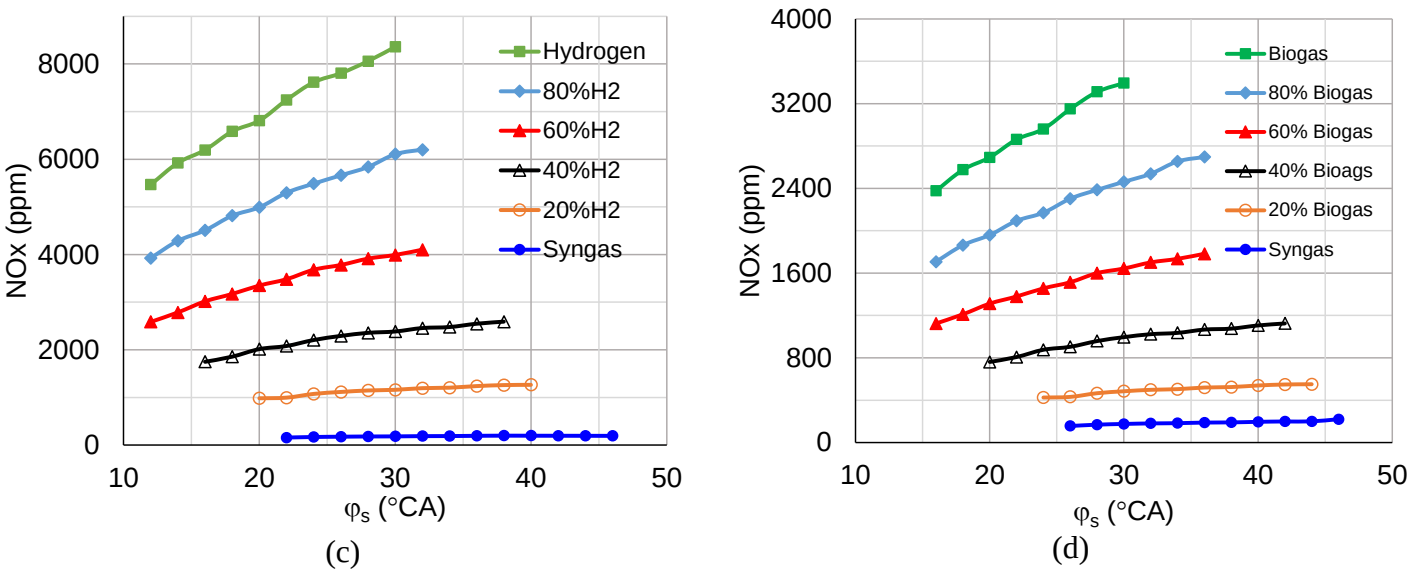

Fig. 11. Effect of biogas and hydrogen compositions in the blend with syngas on the variation of W_i and NO_x with φ_s as the engine operates at 3000rpm with stoichiometric mixture; (a) Variation of W_i with φ_s in case of the syngas-hydrogen blend; (b) Variation of W_i with φ_s in case of the syngas-biogas blend; (c) Variation of NO_x with φ_s in case of the syngas-hydrogen blend; (d) Variation of NO_x with φ_s in case of syngas-biogas blend

With a given content of hydrogen or biogas in the mixture with syngas, the indicative engine work cycle of the engine fueled with a syngas-hydrogen blend is slightly higher and the optimal φ_s is lower than the corresponding values of the engine fueled with the syngas-biogas mixture as shown in **Fig. 11a** and **Fig. 11b**. This is attributed to the fact that hydrogen is a pure fuel with a high combustion rate, while biogas contains impure CO_2 with a low combustion rate [104]. However, under the same comparison conditions, NO_x concentration in the case of a syngas-hydrogen blend is more than double the value of that in the case of syngas-biogas due to the high combustion temperature of the first case.

Fig. 12a and **Fig. 12b** show the variations of φ_{sop}, W_i, and NO_x concentration with the hydrogen and biogas contents in the blend with syngas. The results show that φ_{sop} is 38°CA for syngas, 24°CA for biogas, and 18°CA for hydrogen. When the hydrogen composition varies

from 20% to 90%, φ_{sop} decreases linearly with the hydrogen composition in the blend. Outside this range, φ_{sop} changes rapidly with hydrogen composition. In the case of the syngas-biogas blend, φ_{sop} decreases practically linearly with the biogas content. The maximum indicative engine work cycle reaches 210 J/cyc, 202 J/cyc, and 155 J/cyc for hydrogen, biogas, and syngas, respectively. Thus, when the hydrogen fueling mode is switched to the syngas fueling mode, the derating power is 30%. It is practically the same derating power regarding a switch from natural gas to syngas [53]. With a switch from the biogas fueling mode to the syngas fueling mode, the derating power is 23%. However, NO_x emissions increase very quickly with the hydrogen or biogas content in the syngas. NO_x emission as the engine operates with φ_{sop} increases from 200 ppm (for syngas) to 2800 ppm (for biogas) and over 6000 ppm (for hydrogen). This is because syngas contains many impurities that reduce the combustion temperature.

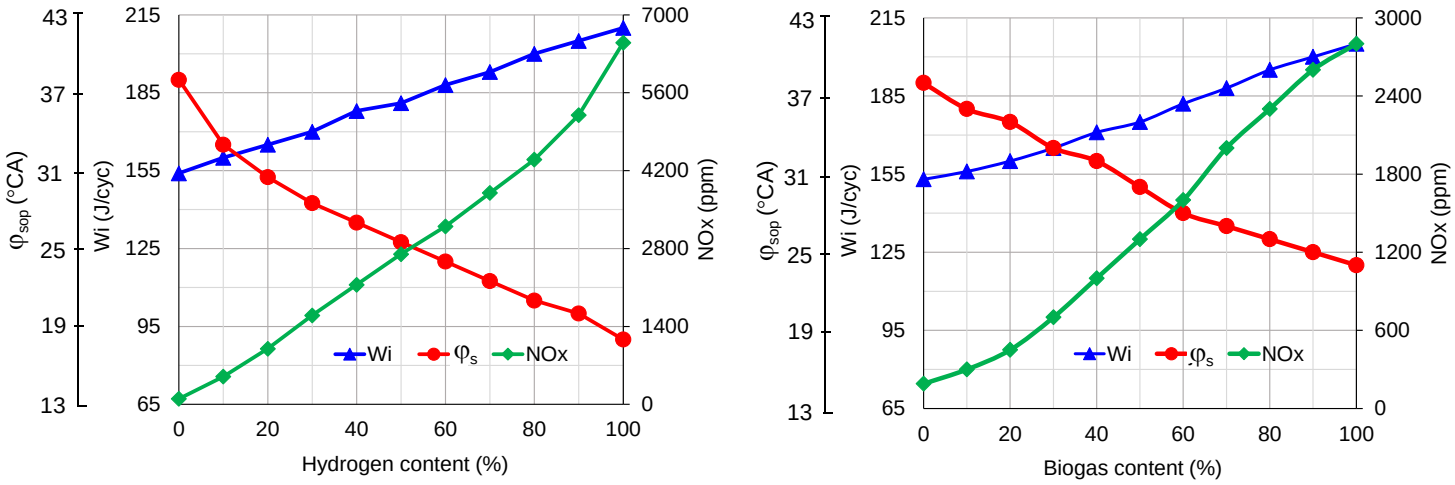

Fig. 12. Variations of W_i, NO_x, and φ_{sop} according to hydrogen content (a) and biogas content (b) in the mixture with syngas (n=3000, $\phi_{optimal}$).

The combined results in **Fig. 13** show that with the same content of hydrogen or biogas in the mixture with syngas, the indicative engine work cycle of the syngas-hydrogen mixture is

about 5 J/cyc larger, but the NO_x concentration is doubled compared to the corresponding values of the syngas-biogas mixture. With the same content of hydrogen or biogas in the blend with syngas, φ_{sop} of the syngas-hydrogen mixture is 4°CA smaller than that of the syngas-biogas mixture. To obtain the same level of NO_x emission, the hydrogen content in the syngas is about 50% of the biogas content in the syngas. Under this condition, the indicative engine work cycle of the syngas-hydrogen fueling mode is about 5 J/cyc less than that of the syngas-biogas fueling mode. In order to achieve the same level of increase in W_i, the biogas content in the syngas is 10% larger than the hydrogen content in the syngas.

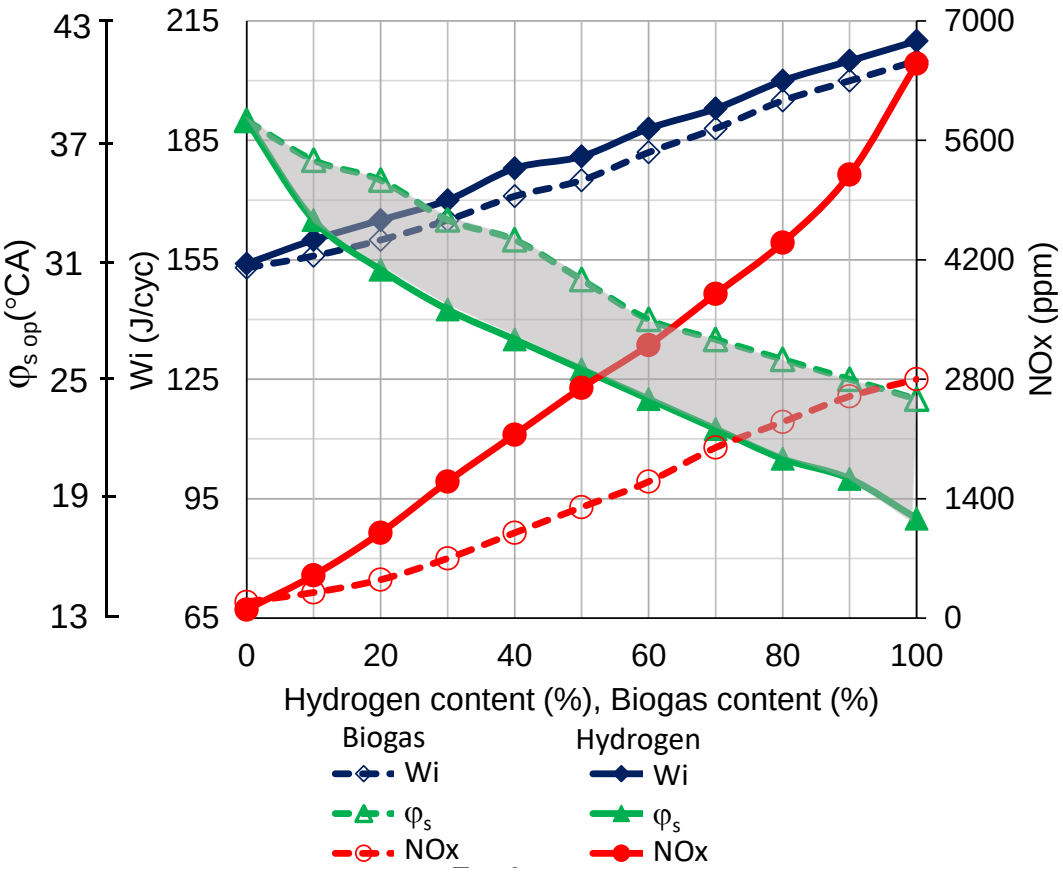

Fig. 13. Variations of W_i, NO_x, and φ_{sop} of the engine fueled with syngas-biogas-hydrogen blends according to hydrogen, and biogas contents in the mixture with syngas (n=3000, $\phi_{optimal}$).

When a syngas-biogas-hydrogen fuel mixture is used, the smallest φ_{sop} is for hydrogen, and the largest φ_{sop} is for syngas. When the syngas component is fixed, φ_{sop} of the syngas-biogas-hydrogen mixture is within the limits of φ_{sop} according to hydrogen content and according to biogas content. φ_{sop} of syngas-biogas-hydrogen blends is thus represented by means of the dark area in **Fig. 13**. φ_{sop} of the syngas-biogas-hydrogen mixture can be adjusted according to the contents of fuel components if gas analysis data is available. In practice, when there is no exact information about the fuel mixture composition, φ_{sop} can be adjusted in the range between its minimum value (corresponding to hydrogen) and its maximum value (corresponding to syngas).

4. Conclusion

The above-mentioned research results enable us to draw out the following conclusions:

- The optimal advanced ignition angle is 38^{o}CA, 24 ^{o}CA, and 18^{o}CA for syngas, biogas, and hydrogen, respectively. With the same content of hydrogen or biogas in the mixture with syngas, the advanced ignition angle of the hydrogen-syngas blend is less than that of the syngas-biogas blend by about 4^{o}CA at the engine speed of 3000 rpm.
- The optimal biogas and hydrogen content in the mixture with syngas is 30% and 20%, respectively. Below these thresholds, W_i increases very fast with biogas or hydrogen content, but exceeding these values, the increase in NO_x concentration is much higher relative to the increase in W_i.
- With a stoichiometric mixture, to obtain the same level of NO_x emission, the hydrogen content in the syngas is about 50% of the biogas content in the syngas. Under this condition, the indicative engine work cycle of the syngas-hydrogen fueling mode is about 5 J/cyc less than that of the syngas-biogas fueling mode. To achieve the same level of increase in Wi, the biogas content in the syngas is 10% larger than the hydrogen content in the syngas.

- When the hydrogen fueling mode is switched to the syngas fueling mode, the derating power is 30%. When the biogas fueling mode is switched to the syngas fueling mode, the derating power is 23%. The NO_x emission increases from 200 ppm (for syngas) to 2800 ppm (for biogas) and to over 6000 ppm (for hydrogen).
- With Blend2, the engine generates the same W_i at full load mode with ϕ=0.8 or at 76% loading mode with $\phi_{optimal}$, but the pollutants emissions of the second case are much higher than those of the first case. The syngas-hydrogen blend is more beneficial than the syngas-biogas blend regarding pollution emission.

The research results show that $\phi_{optimal}$ and φ_{sop} of the stationary engine fueled with a syngas-biogas-hydrogen blend depend on fuel compositions but lie between the respective extreme values for syngas and hydrogen. To improve engine performance and reduce pollutant emissions, the loading control system of the engine should prioritize firstly the adjustment of the equivalence ratio and then the adjustment of the air-fuel mixture flow. A special electronic control unit with flexible adjustment of ϕ and φ_s is needed for the engine working in the solar-biomass HRES.

Acknowledgments:

The authors wish to express their appreciation to the Ministry of Education and Training for supporting this research under project number B2021-DNA-03 "Power generation via RDF produced from solid waste in rural area."

References:

[1] IPCC. 2018/24/PR IPCC PRESS RELEASE. Ipcc 2018:13–6.

[2] Bakır H, Ağbulut Ü, Gürel AE, Yıldız G, Güvenç U, Soudagar MEM, et al. Forecasting of future greenhouse gas emissions trajectory for India using energy and economic indexes with various metaheuristic algorithms. J Clean Prod 2022;360:131946. https://doi.org/10.1016/j.jclepro.2022.131946.

[3] Akarsu B, Serdar Genç M. Optimization of electricity and hydrogen production with hybrid renewable energy systems. Fuel 2022;324:124465. https://doi.org/10.1016/j.fuel.2022.124465.

[4] Rogelj J, Geden O, Cowie A, Reisinger A. Net-zero emissions targets are vague: three ways to fix. Nature 2021;591:365–8. https://doi.org/10.1038/d41586-021-00662-3.

[5] Nguyen XP, Hoang AT, Ölçer AI, Huynh TT. Record decline in global CO2 emissions prompted by COVID-19 pandemic and its implications on future. Energy Sources, Part A Recover Util Environ Eff 2021. https://doi.org/10.1080/15567036.2021.1879969.

[6] Esmaeili Shayan M, Najafi G, Ghobadian B, Gorjian S, Mazlan M. Sustainable design of a near-zero-emissions building assisted by a smart hybrid renewable microgrid. Int J Renew Energy Dev 2022;11:471–80.

[7] Yousefi H, Ghodusinejad MH, Kasaeian A. Multi-objective optimal component sizing of a hybrid ICE + PV/T driven CCHP microgrid. Appl Therm Eng 2017;122:126–38. https://doi.org/10.1016/j.applthermaleng.2017.05.017.

[8] Kakderi C, Komninos N, Panori A, Oikonomaki E. Next City: Learning from cities during COVID-19 to tackle climate change. Sustainability 2021;13:3158.

[9] Hoang AT, Nižetić S, Olcer AI, Chyuan H, Chen W, Chong CT, et al. Impacts of COVID-19 pandemic on the global energy system and the shift progress to renewable energy : Opportunities , challenges , and policy implications. Energy Policy 2021;154:112322. https://doi.org/10.1016/j.enpol.2021.112322.

[10] Guo S, Liu Q, Sun J, Jin H. A review on the utilization of hybrid renewable energy. Renew Sustain Energy Rev 2018;91:1121–47. https://doi.org/10.1016/j.rser.2018.04.105.

[11] Nguyen XP, Le ND, Pham VV, Huynh TT, Dong VH. Mission, challenges, and prospects of renewable energy development in Vietnam. Energy Sources, Part A Recover Util Environ Eff 2021:1–13. https://doi.org/10.1080/15567036.2021.1965264.

[12] Bui VG, Vo TH, Bui TMT, Thi TXN. Characteristics of Biogas-Hydrogen Engines in a Hybrid Renewable Energy System. Int Energy J 2021;21:467–80.

[13] Thellufsen JZ, Lund H, Sorknæs P, Østergaard PA, Chang M, Drysdale D, et al. Smart energy cities in a 100% renewable energy context. Renew Sustain Energy Rev 2020. https://doi.org/10.1016/j.rser.2020.109922.

[14] Krishan O, Suhag S. Techno-economic analysis of a hybrid renewable energy system for an energy poor rural community. J Energy Storage 2019;23:305–19.

[15] Abbassi A, Ben Mehrez R, Abbassi R, Jerbi H, Saidi S, Jemli M. Eco-feasibility study of a distributed power generation system driven by renewable green energy sources. Energy Sources, Part A Recover Util Environ Eff 2022;44:3981–99.

[16] Sharma P, Said Z, Kumar A, Nižetić S, Pandey A, et al. Recent advances in machine learning research for nanofluid-based heat transfer in renewable energy system. Energy & Fuels 2022;36:6626–6658. https://doi.org/10.1021/acs.energyfuels.2c01006.

[17] Li L, Wang X. Design and operation of hybrid renewable energy systems: current status and future perspectives. Curr Opin Chem Eng 2021;31:100669. https://doi.org/10.1016/j.coche.2021.100669.

[18] Salameh T, Sayed ET, Abdelkareem MA, Olabi AG, Rezk H. Optimal selection and management of hybrid renewable energy System: Neom city as a case study. Energy Convers Manag 2021;244:114434.

[19] Jahangir MH, Cheraghi R. Economic and environmental assessment of solar-wind-biomass hybrid renewable energy system supplying rural settlement load. Sustain Energy Technol Assessments 2020;42:100895.

[20] Ilham NI, Hussin MZ, Dahlan NY, Setiawan EA. Prospects and Challenges of Malaysia's Distributed Energy Resources in Business Models Towards Zero–Carbon Emission and Energy Security. Int J Renew Energy Dev 2022;11:1089–100.

[21] Soares J, Oliveira AC. Numerical simulation of a hybrid concentrated solar power/biomass mini power plant. Appl Therm Eng 2017;111:1378–86.

[22] Kumar R, Channi HK. A PV-Biomass off-grid hybrid renewable energy system (HRES) for rural electrification: Design, optimization and techno-economic-environmental analysis. J Clean Prod 2022;349:131347. https://doi.org/10.1016/j.jclepro.2022.131347.

[23] Kaur H, Gupta S, Dhingra A. Analysis of hybrid solar biomass power plant for generation of electric power. Mater Today Proc 2022;48:1134–40. https://doi.org/10.1016/j.matpr.2021.08.080.

[24] Chitsomboon T, Koonsrisook A, Le TH, et al. Experimental investigation of solar energy-based water distillation using inclined metal tubes as collector and condenser. Energy Sources, Part A Recover Util Environ Eff 2021:1–17. https://doi.org/10.1080/15567036.2021.1966139.

[25] Kallio S, Siroux M. Hybrid renewable energy systems based on micro-cogeneration. Energy Reports 2022;8:762–9. https://doi.org/10.1016/j.egyr.2021.11.158.

[26] Shukla AK, Sudhakar K, Baredar P. Renewable energy resources in South Asian countries: Challenges, policy and recommendations. Resour Technol 2017;3:342–6. https://doi.org/10.1016/j.reffit.2016.12.003.

[27] Carlucci AP, Ölçer AI, Ghassemi A, Aghbashlo M, Tabatabaei M, et al. Rice bran oil-based biodiesel as a promising renewable fuel alternative to petrodiesel: A review. Renew Sustain Energy Rev 2021;135:110204. https://doi.org/10.1016/j.rser.2020.110204.

[28] Tulu TK, Atnew SM, Bededa RD, Wakshume DG, Ancha VR. Kinetic Modeling and Optimization of Biomass Gasification in Bubbling Fluidized Bed Gasifier Using Response Surface Method. Int J Renew Energy Dev 2022;11:1043–59.

[29] Huang Z, Nižetić S, Pandey A, Nguyen XP, Luque R, et al. Characteristics of hydrogen production from steam gasification of plant-originated lignocellulosic biomass and its prospects in Vietnam. Int J Hydrogen Energy 2022;47:4394–425. https://doi.org/10.1016/j.ijhydene.2021.11.091.

[30] Shahbaz M, Al-Ansari T, Aslam M, Khan Z, Inayat A, Athar M, et al. A state of the art review on biomass processing and conversion technologies to produce hydrogen and its recovery via membrane separation. Int J Hydrogen Energy 2020;45:15166–95.

[31] Ong HC, Fattah IMR, Chong CT, Cheng CK, Sakthivel R, Ok YS, et al. Progress on the lignocellulosic biomass pyrolysis for biofuel production toward environmental sustainability. Fuel Process Technol 2021;223:106997. https://doi.org/10.1016/j.fuproc.2021.106997.

[32] Arifan F, Abdullah A, Sumardiono S. Effect of Organic Waste Addition into Animal Manure on Biogas Production Using Anaerobic Digestion Method. Int J Renew Energy Dev 2021;10.

[33] Ugwu SN, Enweremadu CC. Enhancement of biogas production process from biomass wastes using iron-based additives: types, impacts, and implications. Energy Sources, Part A Recover Util Environ Eff 2020:1–23.

[34] Li J, Gao C, Lu X, Hoseyni A. A combined energy system consisting of fuel cell, water electrolyzer and solar technologies to produce hydrogen fuel and electricity. Energy Sources, Part A Recover Util Environ Eff 2022;44:1173–88.

[35] Uzal H, Döner A, Bayrakçeken H. Preparation and fabrication of NiCo coated TiO2-NTs for hydrogen evolution. Energy Sources, Part A Recover Util Environ Eff 2022;44:3406–17.

[36] Singh S, Singh M, Kaushik SC. Feasibility study of an islanded microgrid in rural area consisting of PV, wind, biomass and battery energy storage system. Energy Convers Manag 2016;128:178–90. https://doi.org/10.1016/j.enconman.2016.09.046.

[37] Izadi A, Shahafve M, Ahmadi P, Javani N. Transient simulation and techno-economic assessment of a near-zero energy building using a hydrogen storage system and different backup fuels. Int J Hydrogen Energy 2022.

[38] Papatsounis AG, Botsaris PN, Lymperopoulos KA, Rotas R, Kanellia Z, Iliadis P, et al. Operation assessment of a hybrid solar-biomass energy system with absorption refrigeration scenarios. Energy Sources, Part A Recover Util Environ Eff 2022;44:700–17.

[39] Hassan R, Das BK, Hasan M. Integrated off-grid hybrid renewable energy system optimization based on economic, environmental, and social indicators for sustainable development. Energy 2022;250:123823. https://doi.org/10.1016/j.energy.2022.123823.

[40] Hoang AT, Pham VV, Nguyen XP. Integrating renewable sources into energy system for smart city as a sagacious strategy towards clean and sustainable process. J Clean Prod 2021;305:127161. https://doi.org/10.1016/j.jclepro.2021.127161.

[41] Tabak A, Kayabasi E, Guneser MT, Ozkaymak M. Grey wolf optimization for optimum sizing and controlling of a PV/WT/BM hybrid energy system considering TNPC, LPSP, and LCOE concepts. Energy Sources, Part A Recover Util Environ Eff 2022;44:1508–28.

[42] Rajamohan S, Vinod A, Aditya MPVS, Vadivudaiyanayaki HG, Arıcı M, Nižetić S, et al. Approaches in performance and structural analysis of wind turbines–A review. Sustain Energy Technol Assessments 2022;53:102570.

[43] Ağbulut Ü, Aydin M, Karagöz M, Deniz E, Çiftçi B. An experimental assessment of combustion and performance characteristics of a spark ignition engine fueled with co-fermentation biogas and gasoline dual fuel. Proc Inst Mech Eng Part E J Process Mech Eng 2021:09544089211060131.

[44] Nadaleti WC, Przybyla G. Emissions and performance of a spark-ignition gas engine generator operating with hydrogen-rich syngas, methane and biogas blends for application in southern Brazilian rice industries. Energy 2018;154:38–51. https://doi.org/10.1016/j.energy.2018.04.046.

[45] Bui VG, Bui TMT, Nižetić S, Nguyen Thi TX, Vo AV. Hydrogen-Enriched Biogas Premixed Charge Combustion and Emissions in Direct Injection and Indirect Injection Diesel Dual Fueled Engines: A Comparative Study. J Energy Resour Technol 2021;143. https://doi.org/10.1115/1.4051574.

[46] Murugesan P, Perumal Venkatesan E, Santosh Kumar D, Balasubramanian D, et al. Role of hydrogen in improving performance and emission characteristics of homogeneous charge compression ignition engine fueled with graphite oxide nanoparticle-added microalgae biodiesel/diesel blends. Int J Hydrogen Energy 2021. https://doi.org/10.1016/j.ijhydene.2021.08.107.

[47] Hagos FY, Aziz ARA, Sulaiman SA. Trends of Syngas as a Fuel in Internal Combustion Engines. Adv Mech Eng 2014;6:401587. https://doi.org/10.1155/2014/401587.

[48] Hagos FY, Aziz ARA, Sulaiman SA, Mahgoub BKM. Low and Medium Calorific Value Gasification Gas Combustion in IC Engines. Dev. Combust. Technol., InTech; 2016. https://doi.org/10.5772/64459.

[49] Karagöz M, Polat F, Sarıdemir S, Yeşilyurt MK, Ağbulut Ü. An experimental assessment

on dual fuel engine behavior powered by waste tire-derived pyrolysis oil–biogas blends. Fuel Process Technol 2022;229:107177.

[50] Sharma PK, Kumar Sharma A, Shenbagaraj S, Mondal S. An investigation on emissions analysis of spark plug engine fueled by producer gas generated by L. camera. Mater Today Proc 2021;46:11239–42. https://doi.org/10.1016/j.matpr.2021.02.615.

[51] Shah A, Srinivasan R, D. Filip To S, Columbus EP. Performance and emissions of a spark-ignited engine driven generator on biomass based syngas. Bioresour Technol 2010;101:4656–61. https://doi.org/10.1016/j.biortech.2010.01.049.

[52] Pradhan A, Baredar P, Kumar, Anil. Syngas as An Alternative Fuel Used in Internal Combustion Engines: A Review. J Pure Appl Sci Technol 2015;5:51–66.

[53] Sridhar G. Biomass derived producer gas as a reciprocating engine fuel—an experimental analysis. Biomass and Bioenergy 2001;21:61–72. https://doi.org/10.1016/S0961-9534(01)00014-9.

[54] Banapurmath NR, Tewari PG. Comparative performance studies of a 4-stroke CI engine operated on dual fuel mode with producer gas and Honge oil and its methyl ester (HOME) with and without carburetor. Renew Energy 2009;34:1009–15. https://doi.org/10.1016/j.renene.2008.08.005.

[55] Fiore M, Magi V, Viggiano A. Internal combustion engines powered by syngas: A review. Appl Energy 2020;276:115415. https://doi.org/10.1016/j.apenergy.2020.115415.

[56] Chandra R, Vijay VK, Subbarao PMV, Khura TK. Performance evaluation of a constant speed IC engine on CNG, methane enriched biogas and biogas. Appl Energy 2011;88:3969–77. https://doi.org/10.1016/j.apenergy.2011.04.032.

[57] WORLD ECONOMIC FORUM. This is how much rice is produced around the world - and the countries that grow the most 2022.

[58] Ga B Van, Tu BTM. Soot Emission Analysis in Combustion of Biogas Diesel Dual Fuel Engine. Int J Environ Sci Sustain Dev 2017;2:67–79. https://doi.org/10.21625/essd.v1i2.55.

[59] Van Ga B, Van Nam T. Appropriate structural parameters of biogas SI engine converted from diesel engine. IET Renew Power Gener 2014;9:255–61.

[60] Bui VG, Tran VN, Le MT, Bui TMT. Combustion analysis of biogas premixed charge diesel dual fuelled engine 2014.

[61] Hagos FY, A. Aziz AR, Sulaiman SA. Methane enrichment of syngas (H2/CO) in a spark-ignition direct-injection engine: Combustion, performance and emissions comparison with syngas and Compressed Natural Gas. Energy 2015;90:2006–15. https://doi.org/10.1016/j.energy.2015.07.031.

[62] Van Ga B, Van Nam T, Tung TTH. A simulation of effects of compression ratios on the combustion in engines fueled with biogas with variable CO2 Concentrations. J Eng Res Appl Www Ijera Com 2013;3:516–23.

[63] Bui VG, Nguyen VH, Bùi TMT, Van Hung B. Utilization of poor biogas as fuel for hybrid biogas-diesel dual fuel stationary engine 2015.

[64] Kan X, Zhou D, Yang W, Zhai X, Wang C-H. An investigation on utilization of biogas and syngas produced from biomass waste in premixed spark ignition engine. Appl Energy 2018;212:210–22. https://doi.org/10.1016/j.apenergy.2017.12.037.

[65] Makareviciene V, Sendzikiene E, Pukalskas S, Rimkus A, Vegneris R. Performance and emission characteristics of biogas used in diesel engine operation. Energy Convers Manag 2013;75:224–33. https://doi.org/10.1016/j.enconman.2013.06.012.

[66] Khatri N, Khatri KK. Hydrogen enrichment on diesel engine with biogas in dual fuel mode. Int J Hydrogen Energy 2020;45:7128–40. https://doi.org/10.1016/j.ijhydene.2019.12.167.

[67] Jagadish C, Gumtapure V. Experimental investigation of methane-enriched biogas in a single cylinder diesel engine by the dual fuel mode. ENERGY SOURCES PART A-RECOVERY Util Environ Eff 2022;44:1898–911.

[68] Bui VG, Tran VN, Bui TMT, et al. A simulation study on a port-injection SI engine fueled with hydroxy-enriched biogas. Energy Sources, Part A Recover Util Environ Eff 2020. https://doi.org/10.1080/15567036.2020.1804487.

[69] Kim Y, Kawahara N, Tsuboi K, Tomita E. Combustion characteristics and NOX emissions of biogas fuels with various CO2 contents in a micro co-generation spark-ignition engine. Appl Energy 2016;182:539–47.

[70] Van Ga B, Van Nam T, Tu BTM, Trung NQ. Numerical simulation studies on performance, soot and NO x emissions of dual-fuel engine fuelled with hydrogen enriched biogas mixtures. IET Renew Power Gener 2018;12:1111–8.

[71] Rakopoulos CD, Michos CN. Generation of combustion irreversibilities in a spark ignition engine under biogas–hydrogen mixtures fueling. Int J Hydrogen Energy 2009;34:4422–37. https://doi.org/10.1016/j.ijhydene.2009.02.087.

[72] Shivapuji AM, Dasappa S. Influence of fuel hydrogen fraction on syngas fueled SI engine: Fuel thermo-physical property analysis and in-cylinder experimental investigations. Int J Hydrogen Energy 2015;40:10308–28. https://doi.org/10.1016/j.ijhydene.2015.06.062.

[73] Akal D, Öztuna S, Büyükakın MK. A review of hydrogen usage in internal combustion engines (gasoline-Lpg-diesel) from combustion performance aspect. Int J Hydrogen Energy 2020;45:35257–68.

[74] Hoang AT, Pham VV. A study on a solution to reduce emissions by using hydrogen as an alternative fuel for a diesel engine integrated exhaust gas recirculation. AIP Conf. Proc., vol. 2235, AIP Publishing LLC; 2020, p. 20035.

[75] Arroyo J, Moreno F, Muñoz M, Monné C, Bernal N. Combustion behavior of a spark ignition engine fueled with synthetic gases derived from biogas. Fuel 2014;117:50–8. https://doi.org/10.1016/j.fuel.2013.09.055.

[76] Ahmed SA, Zhou S, Tsegay S, Ahmad N, Zhu Y. Effects of hydrogen-enriched biogas on combustion and emission of a dual-fuel diesel engine. Energy Sources, Part A Recover Util Environ Eff 2020:1–16.

[77] Deheri C, Acharya SK, Thatoi DN, Mohanty AP. A review on performance of biogas and hydrogen on diesel engine in dual fuel mode. Fuel 2020;260:116337. https://doi.org/10.1016/j.fuel.2019.116337.

[78] Hu Z, Zhang X. Experimental study on flame stability of biogas / hydrogen combustion. Int J Hydrogen Energy 2019:5607–14. https://doi.org/10.1016/j.ijhydene.2018.08.011.

[79] Acevedo-Arenas CY, Correcher A, Sánchez-Díaz C, Ariza E, Alfonso-Solar D, Vargas-Salgado C, et al. MPC for optimal dispatch of an AC-linked hybrid PV/wind/biomass/H2 system incorporating demand response. Energy Convers Manag 2019;186:241–57.

[80] Bui VG, Bui TMT, Ong HC, Nižetić S, Nguyen TTX, Atabani AE, et al. Optimizing operation parameters of a spark-ignition engine fueled with biogas-hydrogen blend integrated into biomass-solar hybrid renewable energy system. Energy 2022;252:124052. https://doi.org/10.1016/j.energy.2022.124052.

[81] Nadaleti WC, Przybyla G. SI engine assessment using biogas, natural gas and syngas with different content of hydrogen for application in Brazilian rice industries: Efficiency and pollutant emissions. Int J Hydrogen Energy 2018;43:10141–54. https://doi.org/10.1016/j.ijhydene.2018.04.073.

[82] Verhelst S, Wallner T. Hydrogen-fueled internal combustion engines. Prog Energy Combust Sci 2009;35:490–527. https://doi.org/10.1016/j.pecs.2009.08.001.

[83] Park C, Park S, Lee Y, Kim C, Lee S, Moriyoshi Y. Performance and emission characteristics of a SI engine fueled by low calorific biogas blended with hydrogen. Int J Hydrogen Energy 2011;36:10080–8. https://doi.org/10.1016/j.ijhydene.2011.05.018.

[84] Nadaleti WC, Przybyla G. NOx, CO and HC emissions and thermodynamic-energetic efficiency of an SI gas engine powered by gases simulated from biomass gasification under different H2 content. Int J Hydrogen Energy 2020;45:21920–39. https://doi.org/10.1016/j.ijhydene.2020.05.193.

[85] Van Ga B, Tu BTM, Van Dong N, Van Hung B. ANALYSIS OF COMBUSTION AND NOX FORMATION IN A SPARK IGNITION (SI) ENGINE FUELED WITH

HYDROGENHYDROGEN OXYGEN (HHO) ENRICHED BIOGAS. Environ Eng Manag J 2020;19.

[86] The Japan Times. Russia gas crisis highlights Europe's green energy storage problem 2022. https://www.japantimes.co.jp/news/2022/06/10/business/europe-green-energy-storage-problem/ (accessed July 28, 2022).

[87] Climate Home News. Europe's energy crisis offers opportunity to leapfrog towards solar lighting 2022. https://www.climatechangenews.com/2022/07/15/europes-energy-crisis-offers-opportunity-to-leapfrog-towards-solar-lighting/ (accessed July 25, 2022).

[88] Nižetić S, Jurčević M, Čoko D, et al. Implementation of phase change materials for thermal regulation of photovoltaic thermal systems: Comprehensive analysis of design approaches. Energy 2021;228:120546. https://doi.org/10.1016/j.energy.2021.120546.

[89] Liu J, Song R, Nasreen S, et al. Analysis of the complementary property of solar energy and thermal power based on coupling model. Nat Environ Pollut Technol 2019;18:1675–81.

[90] Umana US, Ebong MS, Godwin EO. Biomass production from oil palm and its value chain. J Human, Earth, Futur 2020;1:30–8.

[91] Memon MJ, Memon AR. Wheat straw optimization via its efficient pretreatment for improved biogas production. Civ Eng J 2020;6:1056–63.

[92] McKendry P. Energy production from biomass (part 1): overview of biomass. Bioresour Technol 2002;83:37–46.

[93] Bai Z, Liu Q, Lei J, Wang X, Sun J, Jin H. Thermodynamic evaluation of a novel solar-biomass hybrid power generation system. Energy Convers Manag 2017;142:296–306.

[94] Shkileva A. Implementation of a Degassing System at the MSW Landfill. Civ Eng J 2021;7:1008–14.

[95] Fan J, Hong H, Zhu L, Jiang Q, Jin H. Thermodynamic and environmental evaluation of biomass and coal co-fuelled gasification chemical looping combustion with CO2 capture for combined cooling, heating and power production. Appl Energy 2017;195:861–76.

[96] Varbanov PS, Nižetić S, Sirohi R, Pandey A, Luque R, et al. Perspective review on Municipal Solid Waste-to-energy route: Characteristics, management strategy, and role in circular economy. J Clean Prod 2022;359:131897. https://doi.org/10.1016/j.jclepro.2022.131897.

[97] Indrawan N, Thapa S, Bhoi PR, Huhnke RL, Kumar A. Engine power generation and emission performance of syngas generated from low-density biomass. Energy Convers Manag 2017;148:593–603. https://doi.org/10.1016/j.enconman.2017.05.066.

[98] Solarte-Toro JC, Chacón-Pérez Y, Cardona-Alzate CA. Evaluation of biogas and syngas as energy vectors for heat and power generation using lignocellulosic biomass as raw

material. Electron J Biotechnol 2018;33:52–62.

[99] Abdel-Aal HK, Sadik M, Bassyouni M, Shalabi M. A new approach to utilize hydrogen as a safe fuel. Int J Hydrogen Energy 2005;30:1511–4.

[100] Vargas-Salgado C, Águila-León J, Alfonso-Solar D, Malmquist A. Simulations and experimental study to compare the behavior of a genset running on gasoline or syngas for small scale power generation. Energy 2022;244:122633. https://doi.org/10.1016/j.energy.2021.122633.

[101] Bui VG, Tran VN, Nguyen VD, Nguyen QT, Huynh TT. Octane number stratified mixture preparation by gasoline–ethanol dual injection in SI engines. Int J Environ Sci Technol 2019;16:3021–34. https://doi.org/10.1007/s13762-018-1942-1.

[102] Yousefi A, Guo H, Birouk M. Effect of diesel injection timing on the combustion of natural gas/diesel dual-fuel engine at low-high load and low-high speed conditions. Fuel 2019;235:838–46.

[103] Mahmoodi R, Yari M, Ghafouri J, Poorghasemi K. Effect of reformed biogas as a low reactivity fuel on performance and emissions of a RCCI engine with reformed biogas/diesel dual-fuel combustion. Int J Hydrogen Energy 2021;46:16494–512. https://doi.org/10.1016/j.ijhydene.2020.09.183.

[104] Yu X, Li G, Du Y, Guo Z, Shang Z, He F, et al. A comparative study on effects of homogeneous or stratified hydrogen on combustion and emissions of a gasoline/hydrogen SI engine. Int J Hydrogen Energy 2019;44:25974–84.